Downloaded from specialpapers.gsapubs.org on June 4, 2015

Geological Society of America
Special Paper 369
2003

Evidence for direct mammalian faunal interchange between Europe and Asia near the Paleocene-Eocene boundary

J.J. Hooker
Department of Palaeontology, The Natural History Museum, Cromwell Road, London, SW7 5BD, UK
D. Dashzeveg
Geological Institute, Mongolian Academy of Sciences, Peace Avenue 63, Ulaanbaatar, Mongolia

ABSTRACT

Dispersal of mammals into Europe at the beginning of the Eocene is conventionally interpreted as being solely from North America via the Greenland land bridge, as other routes were apparently unavailable because of the intervention of major seaways. The Tethys separated Europe from Africa to the south, and the West Siberian Sea and Turgai Straits separated Europe from Asia to the east. Using cladistic analysis and paleogeographic reconstructions, three cases of multiple land mammal dispersal across the Turgai Straits from Asia to Europe in the late Paleocene and early Eocene are recognized. Two of these involve the hyopsodontid condylarths *Lessnessina* (with its synonym *Midiagnus,* and including the species *L. khushuensis* sp. nov.) and a *Hyopsodus* clade (*H. orientalis* + *H. itinerans*), which most likely entered Europe early in the Eocene at ~54.5 Ma. The third case is of the order Perissodactyla, whose analysis provides an early history of global dispersal for the group. It indicates that their entry into Europe was earlier than for the hyopsodontids, in the latest Paleocene, perhaps at ~56.5 Ma. As the Turgai Straits are at mid latitudes, not high latitudes like the Bering and Greenland land bridges, it is unlikely that ameliorating climate was the driving force behind these three dispersals. The cause was most likely low sea levels, providing either a narrow land bridge or a greatly narrowed strait, allowing rafting.

INTRODUCTION

At the beginning of the Eocene, dispersal was a major phenomenon, radically affecting mammal faunas in all three Northern Hemisphere continents. This event is known as the Mammalian Dispersal Event (MDE; e.g., Hooker, 2000). Reconstructing dispersal routes and directions is relevant to understanding centers of origin of newly appearing groups. It is thought that the warming event known as the Paleocene-Eocene Thermal Maximum (PETM), associated with the Carbon Isotope Excursion (CIE), was the driving force behind these dispersals. This is because dispersal directions were northwards on northern continents, whereupon the high-latitude Bering and Greenland land bridges became available for intercontinental exchange (e.g., Gingerich, 1989; Clyde and Gingerich, 1998).

Most intercontinental exchange is thought to be via these land bridges, allowing movement between Asia and North America on the one hand and between North America and Europe on the other. However, for much of the Eocene direct land connection between Europe and Asia was interrupted by a major epicontinental seaway, extending from the Arctic Ocean to the Peritethys, known as the West Siberian Sea (Iakovleva et al., 2001) or Obik Sea (McKenna, 1975). This sea narrowed at its southern end at the Turgai Straits. It is widely accepted that no land dispersal took place across this barrier until the Oligocene. In fact, the majority (probably about two thirds) of mammalian

Hooker, J.J., and Dashzeveg, D., 2003, Evidence for direct mammalian faunal interchange between Europe and Asia near the Paleocene-Eocene boundary, *in* Wing, S.L., Gingerich, P.D., Schmitz, B., and Thomas, E., eds., Causes and Consequences of Globally Warm Climates in the Early Paleogene: Boulder, Colorado, Geological Society of America Special Paper 369, p. 479–500. © 2003 Geological Society of America.

Downloaded from specialpapers.gsapubs.org on June 4, 2015

taxa appearing in Europe at the MDE can be readily traced to a North American origin (Hooker, 1998; Beard and Dawson, 1999). Their closest relatives occur only in North America and have in most instances a record in that continent extending back into the Paleocene. Moreover, they have no unequivocal Paleocene record in any other continent. Taxa falling into this category are: the multituberculate *Ectypodus,* peradectid and herpetotheriid marsupials, paramyid rodents, nyctitheriids, oxyaenid creodonts, apatotheres, the tillodont *Esthonyx,* and the "condylarth" genera *Phenacodus* and *Hyopsodus.*

A number of other mammalian taxa have no authenticated Paleocene records anywhere, yet appear around the MDE in North America, Europe and much of Asia. Taxa in this category are: Perissodactyls, artiodactyls, primates, and bats. Hyaenodontid creodonts were formerly also included until their occurrence in the Gashatan Asian Land Mammal Age (ALMA) was demonstrated to be Paleocene (Bowen et al., 2002). The centers of origin for taxa in this category are unknown, although hypothesized at different times to be Africa, Central America, India or other parts of Asia (Gingerich, 1976b, 1989; Hooker, 1998; Krause and Maas, 1990). Although some of these taxa are thought to have dispersed to Europe before moving on to North America, the concept of a direct African or Asian source has been inhibited by the knowledge that the Tethys Ocean and the Turgai Straits respectively formed major long-term barriers to dispersal of land mammals from these continents to Europe.

Critical to Beard and Dawson's (1999) hypothesis that all taxa entering Europe at the MDE came from North America via the Greenland land bridge was the acceptance that no occurrences of these taxa were shared between Europe and Asia exclusive of North America. The present communication documents three such shared occurrences between Europe and Asia, which suggest multiple cases of Asia-Europe interchange with a westerly dispersal direction in the latest Paleocene and earliest Eocene. The method used is cladistic analysis of the taxa concerned, combined with paleogeography (Forey et al., 1992).

Institutional abbreviations

BMNH, Natural History Museum, London; MNHN, Muséum National d'Histoire Naturelle, Paris; UM, University of Michigan Museum of Paleontology; USTL, Université des Sciences et Techniques du Languedoc (Montpellier II).

LESSNESSINA

Lessnessina is an enigmatic mammal genus that was described originally based on upper teeth, from the early Eocene, Neustrian European Land Mammal Age (ELMA), zone PE III site of Abbey Wood, London, UK (Hooker, 1979). Until now it has not been recorded from any other site. However, new finds of a P_4 and an M_2 from Abbey Wood, which occlude well with the uppers, show that the genus *Midiagnus,* described on a lower dentition from the Neustrian PE IV site of Palette, France (Godinot et al., 1987), should be synonymized with *Lessnessina* (Fig. 1). This extends its range to two sites in Europe (see below). A new species of *Lessnessina, L. khushuensis* sp. nov., from the early Eocene Bumbanian site of Tsagan Khushu, Mongolia, extends the range of *Lessnessina* farther from Europe to Asia. The systematics of the three species and the synonymy of *Midiagnus* with *Lessnessina* is established below as a necessary basis for consideration of its dispersal history. Dental terminology follows Hooker (1986).

Systematics

Order "Condylarthra" Cope, 1881
Family Hyopsodontidae Trouessart, 1879
Genus *Lessnessina* Hooker, 1979

Type species: *Lessnessina packmani* Hooker, 1979.

Included species: *Lessnessina praecipuus* (Russell, 1987) comb. nov.; *Lessnessina khushuensis* sp. nov.

Emended diagnosis: Small hyopsodontids, M_2 measuring 2.20–2.55 mm in length. Tooth formula ?/? 1/1 4/4 3/3. P^3-M^2 with "transverse" long axis running slightly distobuccally-mesiolingually. Upper molars with: Centrocrista slightly flexed buccally, meeting mesostyle on M^{1-2}; parastyle not salient buccally. Upper preultimate molars (known only for the type species) with: Protocone massive and with long lingual slope; large metaconule; metacone smaller than paracone. P^{3-4} (known only for the type species) without metacone, massive mesiodistally compressed protocone, taller than paracone, with tall, buccolingually elongate crestiform parastyle and with weak ectocingulum. Lower molars with tall approximated or fused paraconid and metaconid; low entoconid; paracristid with sharp mesiobuccal angle; cristid obliqua joins trigonid at protoconid. P_4 premolariform, without paraconid or metaconid, and with unbasined talonid with single tall terminal cusp.

All other hyopsodontids (sensu herein—see below) have: P^3-M^2 long axis more or less transverse; upper molars with straight centrocrista, smaller metaconule, and equal sized paracone and metacone; lower molars with lower paraconid-metaconid complex, paracristid with rounded mesiobuccal angle, and cristid obliqua with more lingual attachment positions;

Figure 1. Scanning electron micrographs of teeth of species of *Lessnessina,* early Eocene. A–D, F–G, J–K, M–N, *Lessnessina packmani,* Blackheath Beds, Abbey Wood, UK. A, holotype left maxilla with P^2-M^3 (BMNH.M29632); B, paratype right P^4 (reversed) (BMNH.M29756); C, paratype right M^1 (reversed) (BMNH.M44944); D, paratype right M^3 (reversed) (BMNH.M29637); F, J, N, right P_4 (reversed in J and N); G, K, M, right M_2 (reversed in K and M). E, I, O, *Lessnessina khushuensis,* holotype left M_{2-3} (reversed in E) (Geological Institute, Ulaanbaatar, PSS.20–225), Bumban Member, Tsagan Khushu, Mongolia. H, L, P, *Lessnessina praecipuus,* holotype C_1–M_3 (composite of right and left dentitions, shown as right in H, left in L and P) (USTL.PAT7), lignitic marls, Palette, France. Views are occlusal (A–H), buccal (I–L) and lingual (M–P). All images are of gold-coated epoxy casts.

Downloaded from specialpapers.gsapubs.org on June 4, 2015

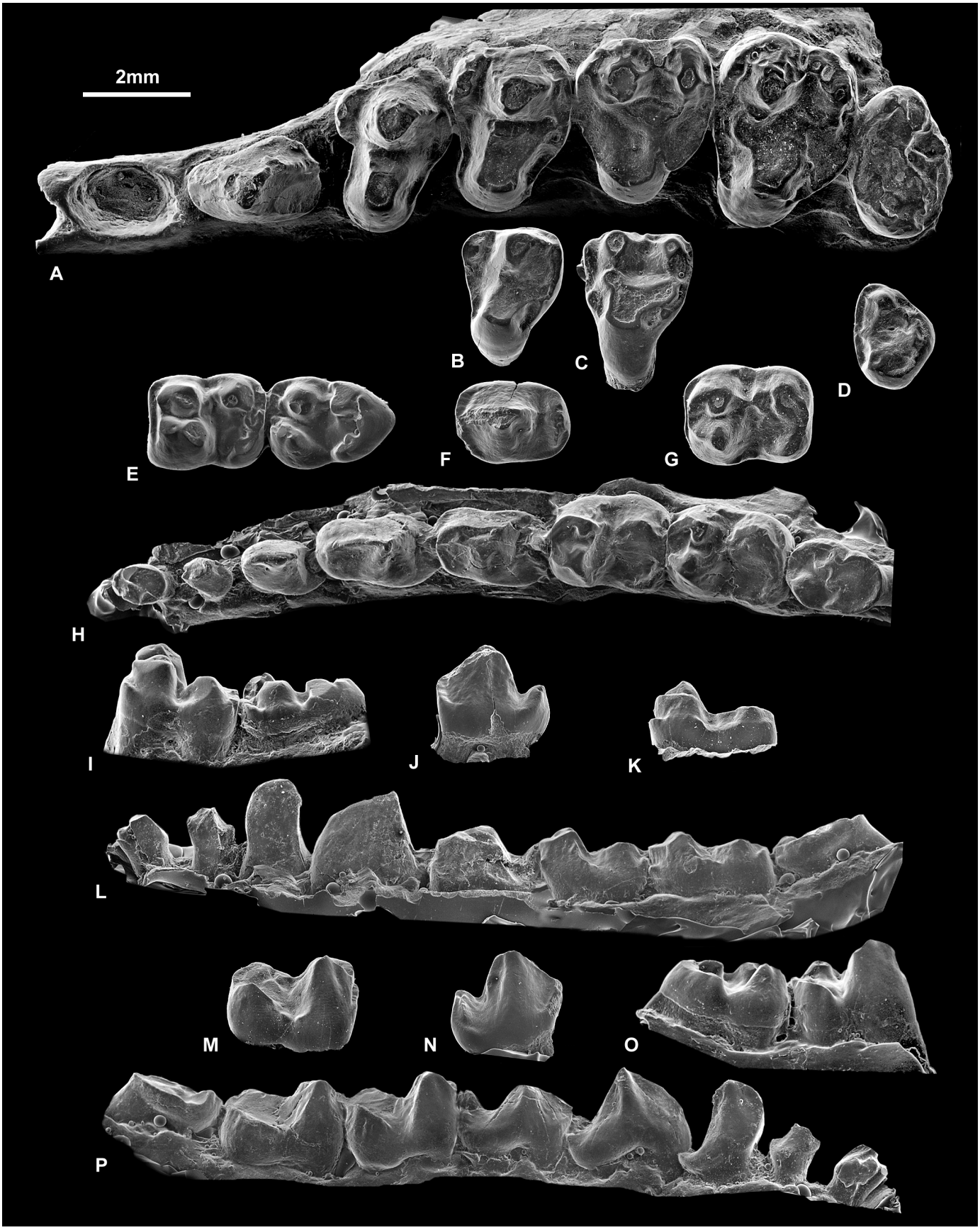

Downloaded from specialpapers.gsapubs.org on June 4, 2015

P^{3-4} with smaller protocones and less buccolingually extensive parastyles; and P_4 with paraconid, metaconid and basined talonid.

All other hyopsodontids apart from *Protoselene* lack an upper molar mesostyle. All except *Haplomylus* and *Hyopsodus* have a buccally salient upper molar parastyle. All have lower upper molar protocones and taller lower molar entoconids except *Litaletes,* where only M^2 has a massive protocone and M_2 a low entoconid. All except *Litaletes* have a lower P_4 talonid. *Haplomylus, Dorraletes,* and *Protoselene* have: Semimolariform fourth premolars with small but distinct P^4 metacone and subterminal P_4 hypoconid; and lower molars with low or absent paraconid. *Hyopsodus* has a much smaller P^4 parastyle.

Synonymy: *Midiagnus* Russell, 1987 is here considered to represent the lower dentition of *Lessnessina* Hooker, 1979, which was until now only known from upper teeth. The former is synonymized with the latter and the reasons given under *L. praecipuus.*

Discussion of family and higher relationships: *Lessnessina* was originally placed in the periptychid "condylarth" subfamily Anisonchinae because of similarity to certain anisonchines in the long lingual slope of the upper molar protocone, upper molar metacone smaller than paracone and large P^3 protocone, the last resembling only *Hemithlaeus* and *Anisonchus* (Hooker, 1979). Subsequent suggestions of relationships have been with the Pseudictopidae or other Anagalida (Archibald et al., 1983, p. 55) or with the order Taeniodonta (Estravis and Russell, 1992).

Now that both upper and lower dentitions of *Lessnessina* are known, new evidence can be brought to bear on this issue. On the basis of the lower teeth, *Lessnessina* is clearly not an anisonchine. Members of the Periptychidae retain the lower molar paraconid quite distinct from the metaconid (Matthew, 1937). Moreover, the entoconid is always a prominent subterminal cusp, and the upper molar precingulum extends to the lingual margin of the tooth. The upper premolar and molar protocone enlargements are thus likely to be convergent with the Anisonchinae.

Regarding possible anagalid relationships, it is true that the strong upper molar pre- and postcingula of *Pseudictops* and *Hsiuannania* superficially resemble those of *Lessnessina* (Xu, 1976; Sulimski, 1969), but here the similarity ends. Pseudictopids have transversely elongate upper molar trigons and lower molars with short low talonids to receive them. There is a strong bilophodonty and this is superimposed on a fundamentally tribosphenic plan. There is no "squaring off" of the lower molars that one finds in *Lessnessina* and other "condylarths." Moreover, the lower molar paraconid has undergone significant reduction with no sign of fusion to the metaconid. Anagalids also show important trends in hypsodonty unlike *Lessnessina.*

With the stem taeniodont *Onychodectes,* there are also superficial similarities to *Lessnessina* in the upper dentition, although major differences are the complete absence of pre- and postcingula and strong reduction of the paraconule and metaconule in the former (Schoch, 1986). Once again the greatest differences are in the lower molars. In *Onychodectes,* there is no sign of a shift of the paraconid toward the metaconid. Like the Anagalida, the lower molars are fundamentally tribosphenic, on which plan increase in height of the talonid and general inflation of cusps are superimposed. There is no "squaring off" as found in "condylarths."

The greatest similarities are in fact between *Lessnessina* and certain members of the Hyopsodontidae, thus following Russell in Godinot et al.'s (1987) familial attribution for *"Midiagnus."* Unfortunately, there is little consensus on content of the family. Various Paleocene genera are usually separated at subfamily or family level as Mioclaeninae or Mioclaenidae (e.g., Simpson, 1937; Williamson, 1996). However, it has been argued that the hyopsodontines *Litomylus* and *Haplaletes* are not even ungulates, and that some mioclaenines are ancestral to some hyopsodontines (Rigby, 1980), raising the issues of paraphyly and polyphyly. The family is clearly in need of thorough revision. Given these problems, to try and establish the relationships of *Lessnessina,* a cladistic analysis is conducted here of *Hyopsodus* plus genera that share with it characters that are unique within "condylarths." These are taxa that are here construed to constitute the family Hyopsodontidae. The characters observed are: A, lower molars with tall paraconid close to or fused with metaconid; B, upper first molar precingulum with protostyle and extending only two thirds to three quarters the distance to the lingual tooth wall; C, P_4 with strong paracristid; D, P_4 with strong distal protoconid crest. *Lessnessina* plus two other genera share all of these characters with *Hyopsodus.* All three species of *Lessnessina* and three species of *Hyopsodus* (see later) have been included in the analysis. Three genera that share some but not all of these characters have also been included. *Protungulatum* is chosen as the outgroup taxon as being the generally accepted most primitive ungulate. The character descriptions are in Appendix 1, the data matrix in Appendix 2. The analysis using PAUP 3.1 (Swofford, 1990) produced two maximum parsimony cladograms of 50 steps, a consistency index excluding uninformative characters of 0.644, and a retention index of 0.758. One result shows an apomorphic *Promioclaenus* branching off below a clade dichotomizing into *Lessnessina* + *Litaletes* and *Hyopsodus.* The other shows a plesiomorphic *Promioclaenus* in a trichotomy with the two clades *Lessnessina* + *Litaletes* and *Hyopsodus.* The strict and majority rule consensus results have the same topology as the second maximum parsimony cladogram, which is shown in Figure 2. It demonstrates paraphyly for the Mioclaenidae, some of the genera included by Archibald (1998) in the family having sister group relationships to different members of the Hyopsodontidae. *Litaletes* is sister taxon to *Lessnessina.* It shares with the latter tall P_4 talonid cusps and a tall M^2 protocone that occludes with an M_2 talonid basin with a reduced entoconid. *Lessnessina* has extended this adaptation to all three molars and raised the height of the paraconid-metaconid complex, thus emphasizing both puncture crush function and the late buccal phase of occlusion (e.g., Butler, 1972). Similar heightening of the protocone on P^{3-4} as well

Downloaded from specialpapers.gsapubs.org on June 4, 2015

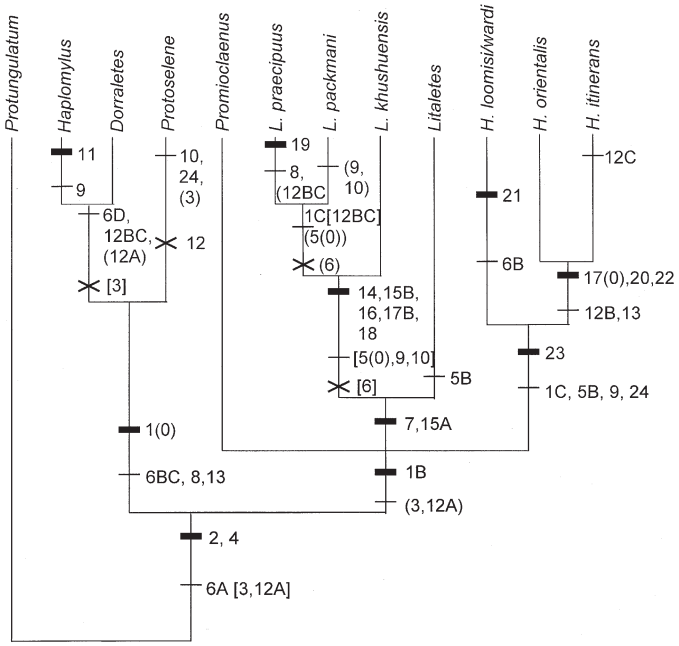

Figure 2. Cladogram of species of *Hyopsodus, Lessnessina,* and their close relatives in the Hyopsodontidae. This is one of two maximum parsimony results, whose topology resembles the strict and majority rule consensuses. Generated by PAUP 3.1 from data matrix in Appendix 2. Broad bar, synapomorphy; narrow bar, normal polarity homoplasy; X, reversal; change to 0 state, where derived, of multistate character indicated by (0). Characters that vary with different optimizations are enclosed between () for DELTRAN and between [] for ACCTRAN. *L.—Lessnessina; H.—Hyopsodus.*

as simple shortening of these teeth is accommodated in the lowers by a simplification, i.e. reduction of the metaconid to a rib on the lingual side of the protoconid and loss of the basin of the talonid.

Lessnessina packmani Hooker, 1979
(Figs. 1A–D, F–G, J–K, M–N, and 3)

v*1979 *Lessnessina packmani* Hooker, p. 50–54, Figure 15.

Holotype: Left maxilla with P^2-M^3, alveolus for P^1 and distal margin of alveolus for canine (BMNH.M29632).

Paratypes: Right P^4 (BMNH.M29756) and right M^1 (BMNH.M44944) possibly associated; right M^3 (BMNH.M29637).

New material: Right dentary fragment with P_4, distal root and mesial alveolus of P_3 and part of alveolus for P_2 (BMNH.M44456); right M_2 (BMNH.M44927).

Horizon and locality: All specimens are from the Lessness Shell Bed, Blackheath Beds, Zone PE III, Neustrian ELMA, early Eocene, Abbey Wood, London, UK.

Emended diagnosis. Lower molars with mesoconid and weak, notched, protocristid; P_4 with mesially sloping paracristid. Like *L. khushuensis* but unlike *L. praecipuus,* lower molars weakly crested, with cuspate entoconid, strong mesial cingulum. Like *L. praecipuus,* but unlike *L. khushuensis,* lower preultimate molar with hypoconulid subsumed by strong posthypocristid, talonid more than half tooth length, postcingulid reduced, and paraconid fused to metaconid; third molar much smaller than second.

***Comparison of new material with* L. praecipuus:** The dentary fragment with P_4 (BMNH.M44456) has a distinctly convex lateral surface and is about twice as deep as the P_4 crown is tall. It shows no sign of shallowing anteriorly to where P_3 was once rooted, and there is a tiny mental foramen below the junction that would have existed between these two teeth, as in *L. praecipuus* (Godinot et al., 1987, pl. 2, figs j–k). There is a slight medial curvature anteriorly but no sign of a symphysis. The P_4 is 2.20 mm long by 1.65 mm wide, thus slightly shorter and broader than that of *L. praecipuus.* It is a simple tooth dominated by a large protoconid with a lingual rib that is slightly less salient than in *L. praecipuus* (Fig. 1F, J, and N). The unicuspid talonid is just over half the height of the slightly tip-worn protoconid and is not as tall as that of *L. praecipuus,* unless the latter is enhanced by the evident damage in this area (Godinot et al., 1987, pl.2, figs h–i). A very faint crest bridges the valley between the talonid and the distal crest of the protoconid. There is a strong precingulid represented on both buccal and lingual sides of the tooth as in *L. praecipuus.* The clearest difference from the latter species is in the angle of slope of the paracristid. This is ~45° in BMNH.M44456, but estimated at ~20°–30° in *L. praecipuus.* The latter has the tip of the protoconid broken and both teeth are slightly worn. However, the slightly greater height of the front of the tooth in *L. praecipuus* versus *L. packmani,* despite heavier wear of the former, testifies to the stronger cresting of the paracristid in *L. praecipuus.*

The M_2 (BMNH.M44927) is 2.55 mm in length, 2.10 mm in trigonid width and 1.95 mm in talonid width, thus relatively very slightly broader than the same tooth in *L. praecipuus.* It is judged to be an M_2 rather than an M_1 because the talonid is slightly narrower than the trigonid. It is very similar morphologically to M_2 in *L. praecipuus,* but differs in the following ways (Fig. 1G, K, and M). The precingulid is slightly stronger. The entoconid is unworn and difficult to compare with the worn one in *L. praecipuus,* but forms a distinct cusp with an entocristid, whereas in the latter there is no obvious buccal salient interrupting the low crest bordering the tooth distolingually. Despite slightly greater tip wear on the protoconid than on the fused paraconid-metaconid, the latter is clearly the taller cusp with a shallower slope lingually than that of the protoconid buccally, so that the paraconid-metaconid tip is nearly at a median point on the tooth when viewed occlusally. Viewed distally, the weak protocristid describes a deep V, meeting the weak buccal cristid obliqua at the base of the distal slope of the protoconid. The talonid basin has a low bump in the middle adjacent to and virtually joining both the mesoconid and hypoconid; the bump bears a lingual phase wear facet on its surface. *L. praecipuus* appears not to have such a bump. It is not clear how significant it is taxonomically, although a similar but slightly more lingually situated one exists in *L. khushuensis* sp. nov.

Downloaded from specialpapers.gsapubs.org on June 4, 2015

Lessnessina praecipuus (Russell, 1987) comb. nov.
(Fig. 1H, L, and P)

v*1987 *Midiagnus praecipuus* Russell in Godinot et al., p. 281, pl. 2, Figures g–k.

Holotype: Associated left and right dentaries with left P_2-M_3 and right canine—M_2 (USTL.PAT7), from lignitic marls between the Calcaire de Langesse and Calcaire de Montaiguet, Zone PE IV, Neustrian ELMA, early Eocene, Palette, Bouches-du-Rhône, France.

Emended diagnosis: Lower molars strongly crested, with crestiform entoconid, strong notched protocristid, and weak mesial cingulum; P_4 with high near horizontal paracristid. Like *L. packmani,* but unlike *L. khushuensis,* lower preultimate molars with paraconid fused to metaconid, hypoconulid subsumed by strong posthypocristid, talonid more than half tooth length, postcingulid reduced; third molar much smaller than second. Like *L. khushuensis,* but unlike *L. packmani,* mesoconid absent.

Reasons for synonymy of Midiagnus with Lessnessina: The new M_2 from Abbey Wood attributed to *Lessnessina packmani* occludes well with the M^1 and M^2 in a unique way (Fig. 3). In the following discussion, wear facets are numbered according to Butler (1973).

Normally in hyopsodontids, the upper and lower molar cusps interlock only in early wear stages. Abrasion quickly produces nearly flat attritional surfaces. In *L. packmani,* the increased height of the upper molar protocone and of the lower molar paraconid-metaconid means that interlocking lasts for more of the life of the teeth (e.g., there is still much relief on M^1 of the holotype even though the enamel pattern of the trigon has been completely worn away). The entoconid, although low, has retreated distally leaving a wide open talonid notch lingually for reception of the protocone. In fact there are large and deep facets on the mesial face of the protocone and distal face of the metaconid, testifying to the majority of translatory wear being late in the buccal phase and predominantly prevallum-postvallid (see e.g., Butler, 1973; Crompton and Kielan-Jaworowska, 1978). In contrast, the wear in early buccal phase is minor, the facets on buccal crests being narrow and difficult to discern except on the upper molar precingulum. Evidence of lingual phase wear is largely obliterated by the heavy cusp tip and crest edge abrasion caused by puncture crush. However, it can be best seen on the M_2, where the protocone of M^2 has produced lingual phase facets (10) on the lingual edges of the mesoconid, hypoconid, posthypocristid and raised bump in the talonid basin. It is the postcingulum of M^1 on the other hand that has produced the lingual phase facets on the lingual edge of the M_2 paracristid (5). A group of facets have an angle intermediate between the buccal and lingual phase ones. They are labeled here with Greek letters. They imply a short intermediate phase between the buccal and lingual.

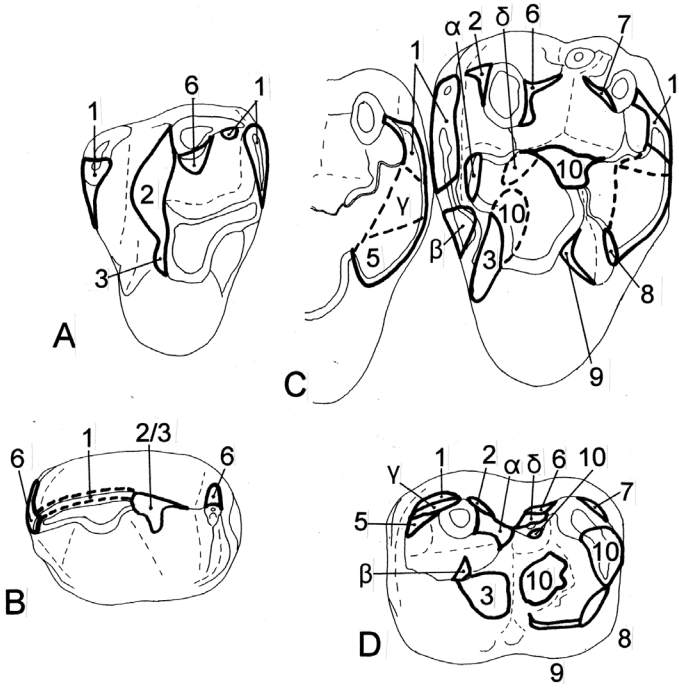

Figure 3. Wear facets of upper (A) and lower (B) fourth premolars and upper first (part) and second (C) and lower second (D) molars of *Lessnessina packmani,* demonstrating matching occlusion of "*Midiagnus,*" based on lowers, with *Lessnessina,* based on uppers. Numbering system for buccal and lingual phase facets follows Butler (1973). Greek letters used for upper and lower homologous molar facets of intermediate angle between buccal and lingual as discussed in text.

Occlusion between P_4 and P^4 is best seen on *L. packmani* specimens M44456 and M44944 respectively. On the P^4, a large facet extends on the mesial face from the paracone to the protocone, via the preprotocrista that links the two cusps (2–3). The large parastyle wraps over the protoconid tip and bears an extensive facet (1). The postparacrista, metacingulum and possibly the short postprotocrista of P^3 make contact with the P_4 paracristid, whilst the P^3 paracone makes a very small area of contact with the P_4 precingulid (6). These $P^{3–4}$ facets make contact only with the longitudinal crest edge of the P_4 trigonid. The lingual margin of the P^4 paracone bears a facet, which occludes with one on the buccal face of the P_4 talonid cusp (6). There is no evidence of lingual phase wear on the premolars. The main function of the massive $P^{3–4}$ protocone is thus mainly puncture crushing.

The P_4 and M_2 of *Midiagnus praecipuus* are so similar to those of *Lessnessina packmani* as to leave little doubt as to the congeneric status of the two, *Lessnessina* having priority. The entire lower tooth rows of *Midiagnus* provide a pattern of cusps, crests and facets that make for accurate occlusal matching with *Lessnessina.* The only differences are minor ones of degree of cresting etc., as borne out in the specific diagnoses. The upper molars of *L. praecipuus,* if found, would be expected to have a more buccally flexed centrocrista, which, together with the postmetacrista and preprotocrista, would also be more strongly crested.

Direct manipulated occlusion between the holotype dentitions of *L. packmani* and *L. praecipuus* is not strictly possible because of slight size differences and because of diagenetic foreshortening and offsetting of some of the teeth of the latter. How-

Downloaded from specialpapers.gsapubs.org on June 4, 2015

ever, in addition to the distal premolar and preultimate molar occlusion already discussed, it can be seen that the long high P_3 paracristid of *L. praecipuus* matches well with the long P^2 postparacrista of *L. packmani*. Also, the reduced M_3 of *L. praecipuus* fits well against the similarly reduced M^3 of *L. packmani.*

Lessnessina khushuensis sp. nov.
(Fig. 1E, I, and O)

Holotype: Left dentary fragment with $M_{2–3}$ (Geological Institute, Ulaanbaatar, PSS.20–225) from the base of the Bumban Member, Naran Bulak Formation, Bumbanian, early Eocene, Tsagan Khushu, near Naran Bulak, Mongolia.

Etymology: Named for the type locality Tsagan Khushu.

Diagnosis: Lower molars with paraconid separate from metaconid; lower preultimate molars with distinct hypoconulid and weak posthypocristid; talonid less than half tooth length; postcingulid strong, joining hypoconulid, protocristid absent; third molar subequal in size to second molar. Like *L. packmani,* but unlike *L. praecipuus,* lower molars weakly crested, with cuspate entoconid, and strong mesial cingulum. Like *L. praecipuus,* but unlike *L. packmani,* lower molar mesoconid absent.

Description and comparisons: M_2 is 2.20 mm in length, 1.80 mm in trigonid width and 1.75 mm in talonid width. M_3 is 2.30 mm in length, 1.70 mm in trigonid width and 1.50 mm in talonid width. Most of the morphological features are covered in the diagnosis. Additional points are made here. The teeth are moderately worn, but the trigonid cusps seem to be taller than those of either *L. packmani* or *L. praecipuus.* Certainly, there is less overhang of the protoconid by the paraconid-metaconid complex. In M_2 the weak cristid obliqua is bowed buccally, notched in the middle and joins the trigonid at the back of the protoconid. There is an obliquely orientated low bump in the talonid basin, behind the metaconid but close to the entoconid, similar to *L. packmani.*

M_3 is difficult to compare with the other species. The tooth type is otherwise only known in *L. praecipuus,* where heavy wear has removed most features, and is most easily interpreted by comparison with *L. khushuensis.* The cusps are all lower than on M_2. The protoconid and paraconid-metaconid complex are more widely separated than on M_2 and the deep valley separating them passes uninterrupted into the talonid basin. The weak paracristid descends steeply to the mesial tooth margin to meet a strong precingulid. The paraconid and metaconid are only separated at their tips. A bump in the talonid basin is situated between the hypoconid and entoconid and has a narrow link to the latter. The hypoconulid is a weak cusp on the distally bowed postcristid, which forms only a slightly bulging hypoconulid lobe. The *L. praecipuus* M_3 is similar in structure, but differs mainly in having an accessory crest trending toward but stopping short of the metaconid.

Dispersal route and direction

There is no record of the genus *Lessnessina* from the well-sampled early Eocene deposits of North America. This indicates direct interchange between Europe and Asia without the intervention of North America, implying that the Turgai Straits were the dispersal route.

To establish direction, it is necessary to orient the relevant part of the cladogram in Figure 2 on a paleogeographic map. The nearest sister taxon to *Lessnessina* is the North American Paleocene genus *Litaletes. Litaletes* has M_3 and M_2 subequal and a paraconid on M_2 and M_3. Therefore, *L. packmani* and *L. praecipuus* are more derived than *L. khushuensis* sp. nov. in having fused the lower molar paraconid and metaconid, and reduced the size of M_3 (Fig. 2). *L. khushuensis* may have some autapomorphies preventing it from being a candidate for direct ancestry of the European species. However, individual variation cannot be assessed and principal character polarity suggests dispersal from east to west (Fig. 4).

HYOPSODUS

Our second example involves the hyopsodontid *Hyopsodus* Leidy, 1870. This genus occurs in the early Eocene in North America, Asia and Europe. It was cited in the Introduction as an example of an immigration into Europe from North America, on the basis of a first occurrence in the late Clarkforkian North American Land Mammal Age (NALMA) of the Bighorn Basin, Wyoming, USA (Rose, 1981). Europe contains two species, *H. wardi* Hooker, 1979 from the London and Paris Basins and *H. itinerans* Godinot, 1978 from the southern French site of Rians. Both are similarly small, but morphologically rather different from one another as noted by Godinot (1981). Compared to *H. wardi, H. itinerans* is more strongly crested, has an M_3 smaller than M_2, $M_{1–2}$ hypoconulid slightly closer to the entoconid, smaller P_4 with shorter, narrower talonid, and no lower molar entocristid. It shares these characters with *H. orientalis* Dashzeveg, 1977 from the Bumbanian ALMA of Tsagan Khushu, near Naran Bulak, Mongolia (Figs. 6–9). In contrast, *H. wardi* is morphologically very similar to the slightly larger, earliest and most primitive North American species, *H. loomisi* McKenna, 1960 (Figs. 5–8). Upper teeth are less well known for *H. itinerans,* but *H. orientalis* has a similarly reduced M^3 and a mesiodistally shorter P^4 with projecting parastyle, which occlusally matches the short talonid of P_4 (Figs. 5E–G, 6G). The considerable transverse width of M^2 in *H. itinerans* may be an autapomorphy of this species (Fig. 5F).

It should be noted that species of *Hyopsodus* are notoriously variable intraspecifically in morphology (Redline, 1997), and contemporaneous North American species are usually distinguished on size (e.g., Gingerich, 1976a). In fact, in the large assemblages of North American species, it is possible to find variants with one or several of the characters of the Eurasian *H. itinerans* and *H. orientalis,* although these are uncommon. *H. itinerans* and *H. orientalis* are consistent for their defining characters (Godinot, 1981; Kondrashov and Agadjanian, 1999), and, even though assemblage sizes are small, the character states represented are likely to be in the vicinity of the mode, not at the

Downloaded from specialpapers.gsapubs.org on June 4, 2015

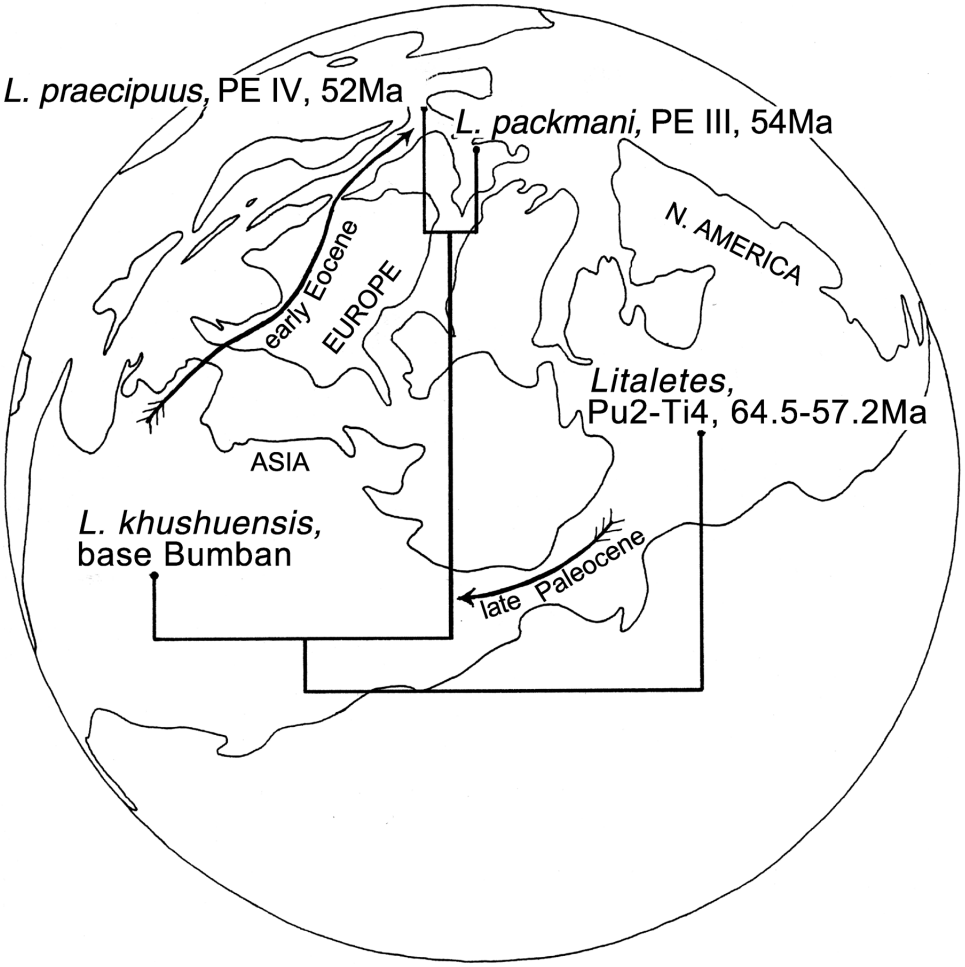

Figure 4. Early Eocene polar projection Northern Hemisphere paleogeographic shoreline map, with superimposed cladogram of *Lessnessina* species from Figure 2 with zones, time ranges in Ma where known and proposed dispersal directions (arrows) (map from unpublished work by Paul Markwick, see Markwick et al., 2000, with minor modifications to North Sea–Arctic Ocean link following Iakovleva et al., 2001).

margins of variation. Figure 9 shows lengths and widths of M_2 and M_3 in the four species concerned. The values for M_3 of *H. itinerans* and *H. orientalis* lie well outside the range of the large assemblage of *H. loomisi* from Wa0 (Gingerich, 1989), whereas those for M_2 nearly coincide. Therefore, *H. itinerans* and *H. orientalis* consistently have relatively smaller lower third molars than do *H. loomisi* or *H. wardi.*

The many other species of North American *Hyopsodus* are not considered here as they are recognized to be derivatives of *H. loomisi* (Gingerich, 1974, 1976a, 1985; Redline, 1997). All are more derived than *H. wardi, H. itinerans* or *H. orientalis* in features such as large M^{1-2} hypocone, hypocone on M^3, and fusion of M_{1-2} paraconid to metaconid. Their relationships are thus judged to be relatively remote from *H. itinerans* or *H. orientalis.*

The cladogram in Figure 2 shows southern French *H. itinerans* to be more closely related to Asian *H. orientalis* than to southern English *H. wardi* and North American *H. loomisi,* which were combined for the analysis. In fact, *H. wardi* is only distinguishable from *H. loomisi* on size (Fig. 9; Hooker, 1979; Gingerich, 1989). On the basis of both an extensive and diverse North American Paleocene record of the family Hyopsodontidae and of the earliest record of the genus *Hyopsodus* being from that continent, one can envisage initial dispersal from North America, probably at the beginning of the Eocene, in two directions. One of these was to Asia via the Bering Straits and the other to northern Europe via Greenland. Speciation followed with subsequent dispersal from Asia to central Europe via the Turgai Straits a little later in the early Eocene and at least by Zone PE III time (Fig. 10).

PERISSODACTYLS

The first two examples discussed here are members of a family that has a known record back through most of the Paleocene. Our third example relates to an order that is not certainly known before the Eocene and has no very close relatives in the Paleocene and thus no clear center of origin. A cladistic analysis of the most primitive members of the order and of their closest nonperissodactyl relatives is carried out here. Their relationships in terms of paleobiogeography provide a hypothesis on the nature and place of their origins and subsequent dispersal.

Downloaded from specialpapers.gsapubs.org on June 4, 2015

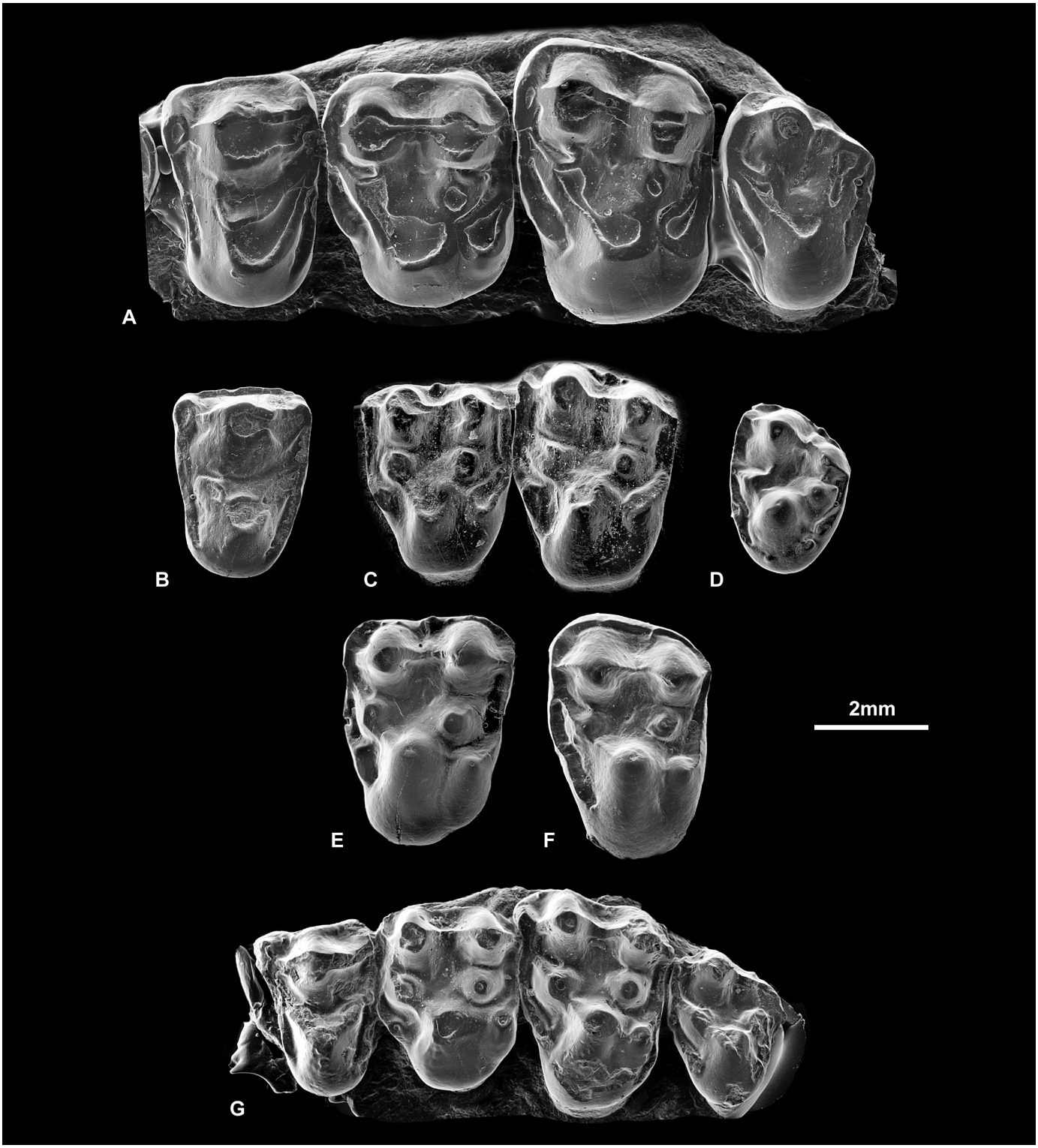

Figure 5. Scanning electron micrographs of occlusal views of upper cheek teeth of species of *Hyopsodus,* early Eocene. A, *Hyopsodus loomisi,* left P^4-M^3 (UM.63620), Willwood Formation, locality 383, Bighorn Basin, Wyoming, USA. B–D, *Hyopsodus wardi,* Blackheath Beds Abbey Wood, UK; B, paratype left P^4 (BMNH.M44946); C, holotype right M^{1-2} (reversed) (BMNH.M29762); D, paratype right M^3 (reversed) (BMNH.M29644). E–F, *Hyopsodus itinerans,* Sables Bleutés, Rians, France; E, holotype left M^1 (MNHN.RI 279); F, right M^2 (reversed) (MNHN.RI 157). G, *Hyopsodus orientalis,* left P^4-M^3 (Geological Institute, Ulaanbaatar, PSS 20–226), Bumban Member, Tsagan Khushu, Mongolia. All images are of gold-coated epoxy casts.

Downloaded from specialpapers.gsapubs.org on June 4, 2015

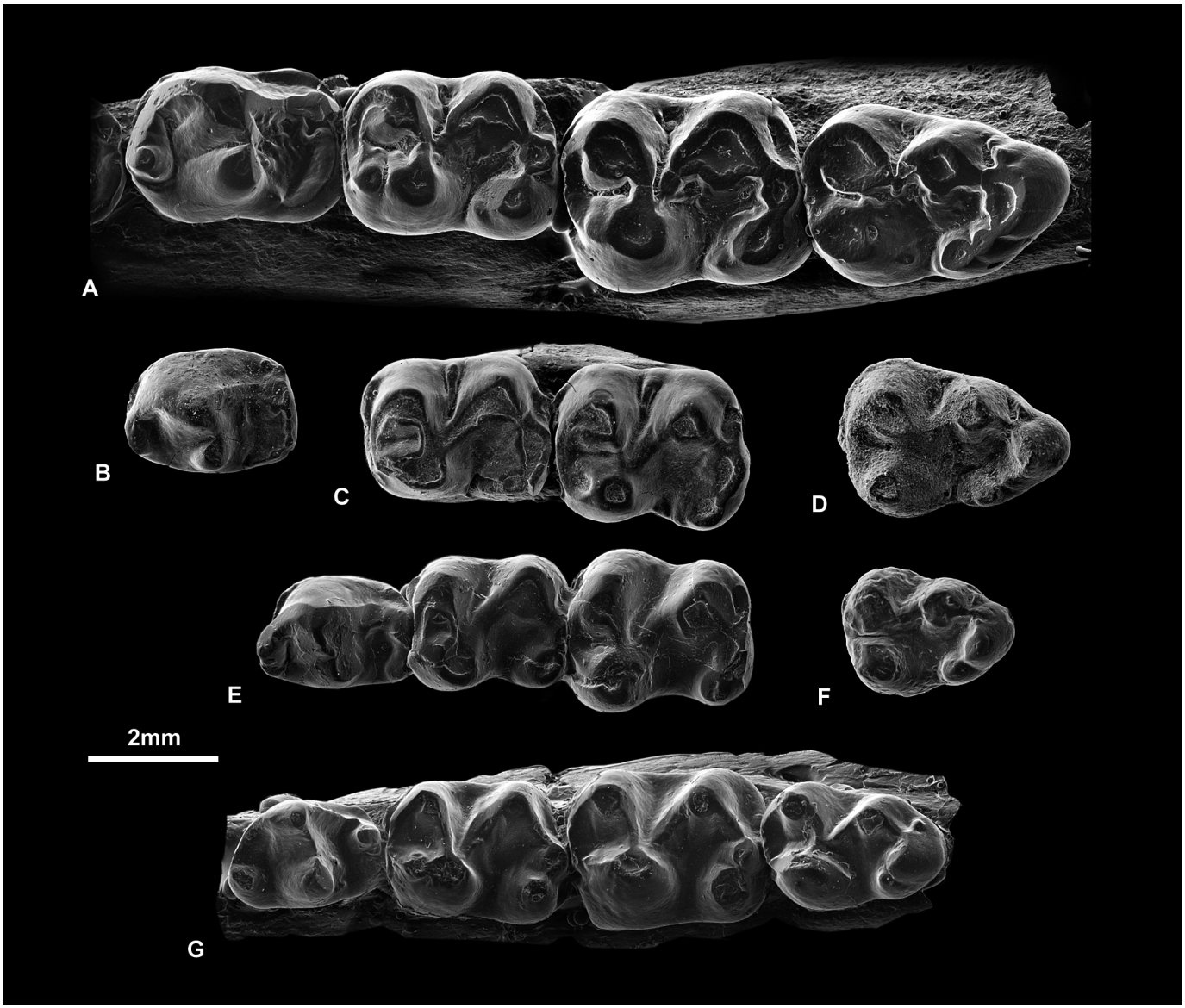

Figure 6. Scanning electron micrographs of occlusal views of lower cheek teeth of species of *Hyopsodus,* early Eocene. A, *Hyopsodus loomisi,* right P_4-M_3 (UM.63621), Willwood Formation, locality 383, Bighorn Basin, Wyoming, USA. B–D, *Hyopsodus wardi,* Blackheath Beds, Abbey Wood, UK; B, paratype right P_4 (BMNH.M29757); C, paratype right $M_{1–2}$ (BMNH.M15146); D, paratype right M_3 (BMNH.M15132). E–F, *Hyopsodus itinerans,* Sables Bleutés, Rians, France; E, left P_4-M_2 (reversed) (original Loggia Collection, cast BMNH.M42629); F, right M_3 (MNHN.RI 280). G, *Hyopsodus orientalis,* paratype left P_4-M_3 (reversed) (Geological Institute, Ulaanbaatar, PSS.20–46), Bumban Member, Tsagan Khushu, Mongolia. All images are of gold-coated epoxy casts.

Methods

The list of taxa includes several relatively recently described Asian genera. Three phenacodontid genera, *Ectocion, Lophocion* and *Phenacodus,* are also included in the analysis (Appendix 4). The last of these is used as the outgroup, for which some justification needs to be made.

The Chinese genus *Radinskya* has been suggested as an outgroup for perissodactyls because of its incipient perissodactyl-like bilophodonty (McKenna et al., 1989; Beard, 1998; Froehlich, 1999). Although only upper teeth are known for *Radinskya,* these show more similarity to phenacolophids than to perissodactyls. Examples of the relevant derived characters involve the upper molars: Crestiform parastyle; and tall metaconule close to the hypocone, lying exactly on a line drawn between the metacone and hypocone. The perissodactyl-like bilophodonty is, however, more similar to derived members of the suborder Ceratomorpha, than to primitive perissodactyls

Downloaded from specialpapers.gsapubs.org on June 4, 2015

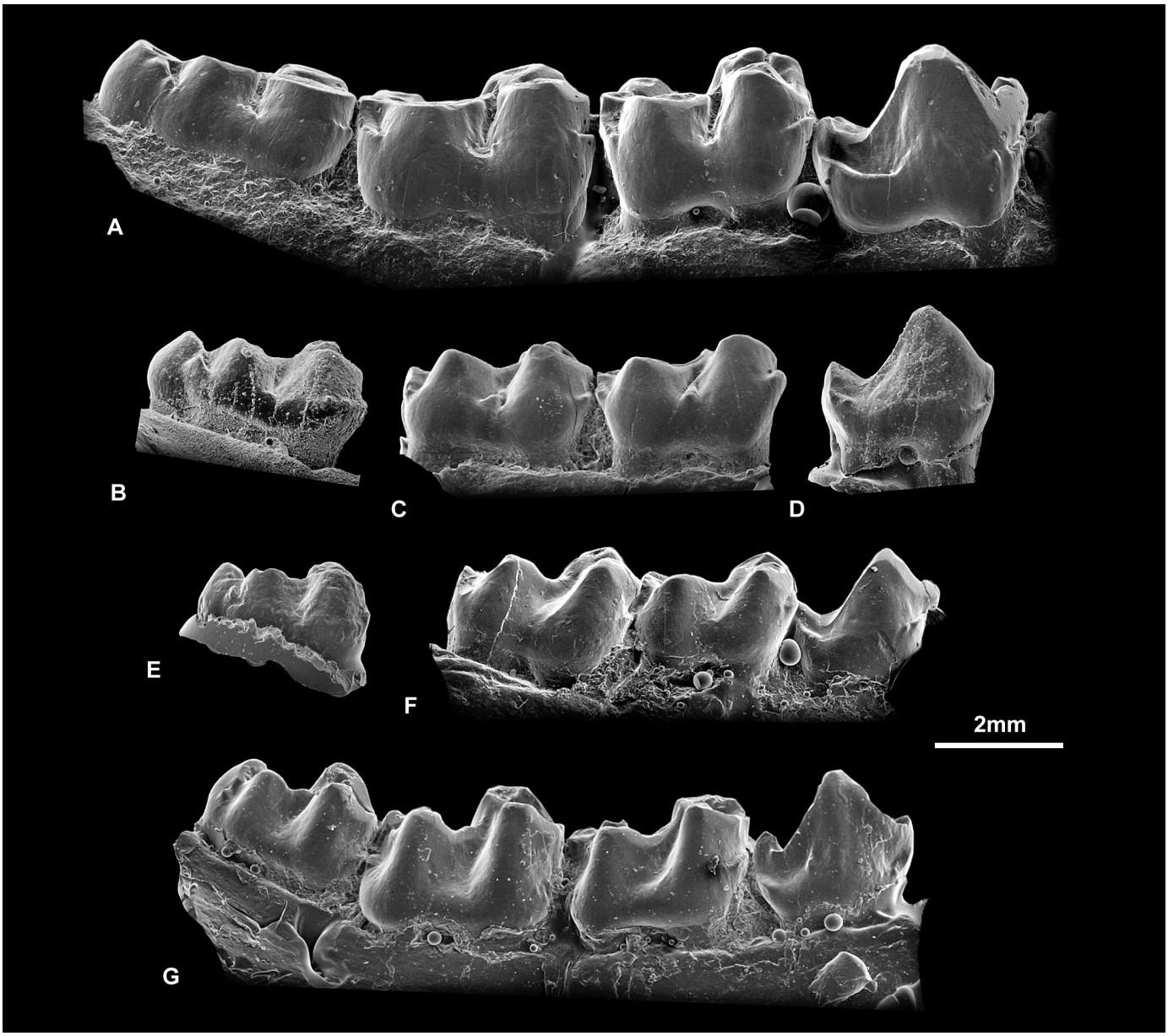

Figure 7. Scanning electron micrographs of buccal views of lower cheek teeth of species of *Hyopsodus,* early Eocene. A, *Hyopsodus loomisi,* right P_4-M_3 (UM.63621), Willwood Formation, locality 383, Bighorn Basin, Wyoming, USA. B–D, *Hyopsodus wardi,* Blackheath Beds, Abbey Wood, UK; B, paratype right M_3 (BMNH.M15132); C, paratype right $M_{1–2}$ (BMNH.M15146); D, paratype right P_4 (BMNH.M29757). E–F, *Hyopsodus itinerans,* Sables Bleutés, Rians, France; E, right M_3 (MNHN.RI 280); F, left P_4-M_2 (reversed) (original Loggia Collection, cast BMNH.M42629). G, *Hyopsodus orientalis,* paratype left P_4-M_3 (reversed) (Geological Institute, Ulaanbaatar, PSS.20–46), Bumban Member, Tsagan Khushu, Mongolia. All images are of gold-coated epoxy casts.

where the metaloph is based around a small, mesially shifted metaconule. Phenacodontids, on the other hand, have long been regarded as close relatives of perissodactyls because of phenetic similarity (e.g., Radinsky, 1966), although also to other pantomesaxonians (Thewissen and Domning, 1992). *Phenacodus* is a relatively generalized member of the family and for that reason is chosen here as outgroup.

The 39 characters and the descriptions of their states are listed in Appendix 3. They are slightly modified from those used solely for equoids by Hooker (1994). As in this last work, they frequently combine characters of upper and lower teeth that are linked by occlusal relationships in an attempt to reduce the incidence of inadvertent weighting. Characters that are judged to form transformation series are treated as ordered and

Downloaded from specialpapers.gsapubs.org on June 4, 2015

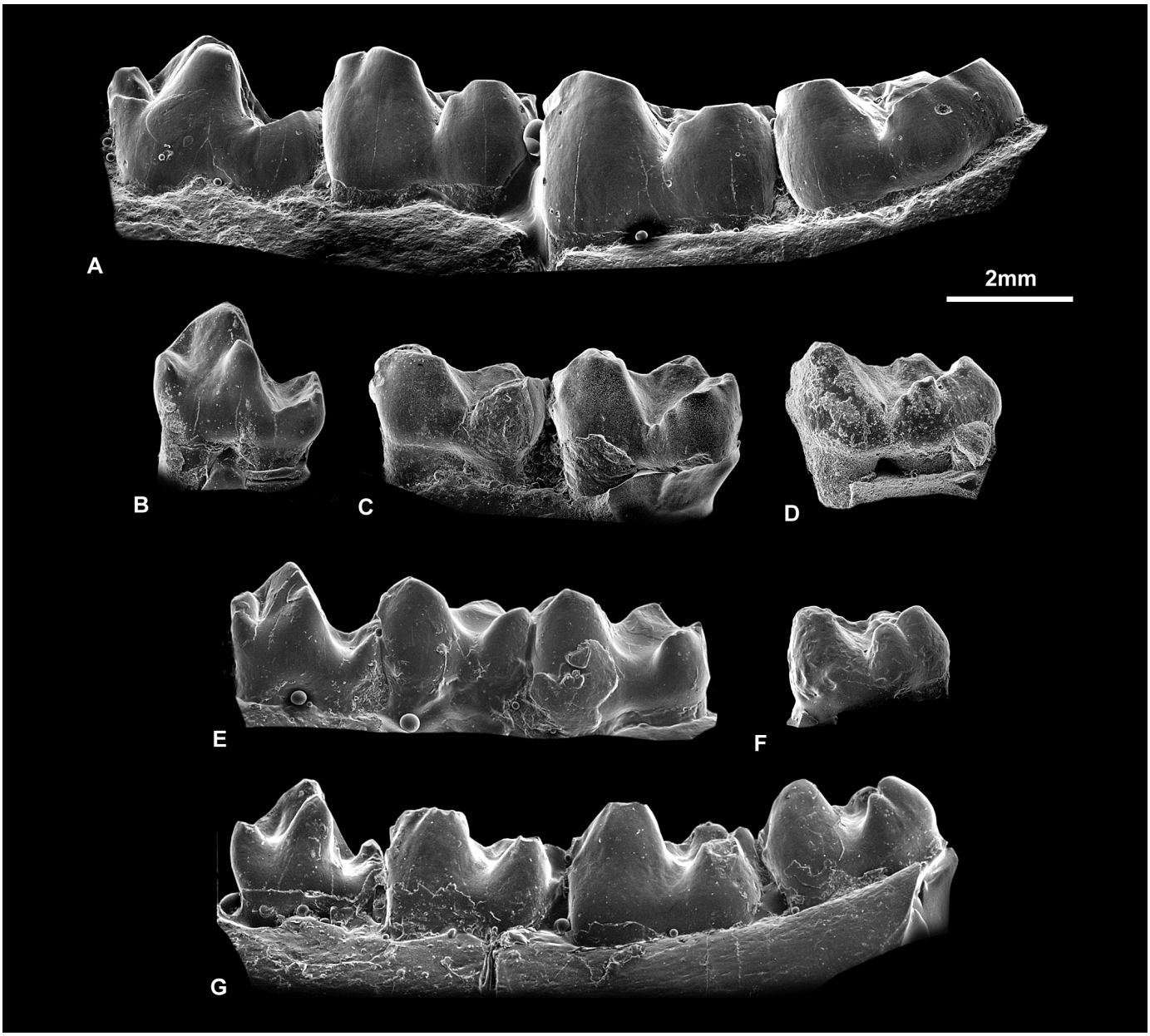

Figure 8. Scanning electron micrographs of lingual views of lower cheek teeth of species of *Hyopsodus,* early Eocene. A, *Hyopsodus loomisi,* right P_4-M_3 (UM.63621), Willwood Formation, locality 383, Bighorn Basin, Wyoming, USA. B–D, *Hyopsodus wardi,* Blackheath Beds, Abbey Wood, UK; B, paratype right P_4 (BMNH.M29757); C, paratype right $M_{1–2}$ (BMNH.M15146); D, paratype right M_3 (BMNH.M15132). E–F, *Hyopsodus itinerans,* Sables Bleutés, Rians, France; E, left P_4-M_2 (reversed) (original Loggia Collection, cast BMNH.M42629); F, right M_3 (MNHN.RI 280). G, *Hyopsodus orientalis,* paratype left P_4-M_3 (reversed) (Geological Institute, Ulaanbaatar, PSS.20–46), Bumban Member, Tsagan Khushu, Mongolia. All images are of gold-coated epoxy casts.

some are entered as stepmatrices to reduce or avoid duplication and consequent potential weighting of primitive states (Lipscomb, 1992). Characters are dominantly dental because of the limited representation of other parts of the anatomy in these early perissodactyls.

Results

The data matrix in Appendix 4 was analyzed using PAUP 3.1 (Swofford, 1990) and resulted in three maximum parsimony cladograms of 100 steps, with a consistency index excluding un-

Downloaded from specialpapers.gsapubs.org on June 4, 2015

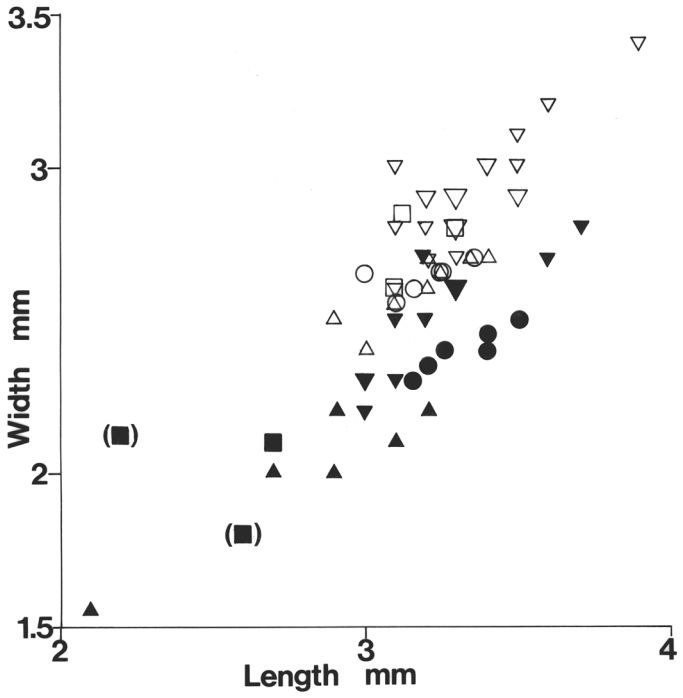

Figure 9. Scatter diagram of length versus width in millimeters of second and third lower molars of species of *Hyopsodus.* ○—*H. wardi,* □—*H. itinerans,* △—*H. orientalis,* ∇—*H. loomisi.* Hollow symbol—second molar, solid symbol—third molar. Three successive increasing sizes of inverted triangle symbol indicate 1, 2, and 3 coincident plots respectively. Bracketed symbols indicate estimated measurements. Plots of *H. orientalis* partly taken from measurements in Kondrashov and Agadjanian (1999). Those of *H. loomisi* from measurements provided by P.D. Gingerich.

informative characters of 0.600 and a retention index of 0.746 (Fig. 11). All three topologies show *Ectocion* and *Lophocion* branching off successively from the outgroup. *Lophocion,* with its incipient metaloph and reduced metaconule on upper molars is a step nearer perissodactyls than is *Ectocion.* Both these phenacodontids have bulbous upper molar parastyles like those of perissodactyls, and ones that are enlarged over those of *Phenacodus.* They are morphologically unlike those of *Radinskya.*

All three topologies also show *Lambdotherium* and its sister taxon *Danjiangia* branching off next. *Danjiangia* was described as a primitive chalicothere by Wang (1995). *Danjiangia* lacks the complete high upper premolar and upper molar metaloph joining the ectoloph, and the absence of upper molar mesostyle of primitive chalicotheres such as *Paleomoropus* and *Lophiaspis* (Radinsky, 1964; Depéret, 1910; Savage et al., 1966). In contrast, it has the strong dilambdodonty (especially the buccally deflected upper molar preparacrista) of *Lambdotherium* (e.g., Osborn, 1929).

Above this node, topologies fall into two main categories, those that show equoids to be paraphyletic (Fig. 11B–C) and that which shows them to be monophyletic (Fig. 11A). The paraphyletic alternatives differ in the relationships of *Karagalax* plus *Pachynolophus* to *Orientolophus* and *Cardiolophus.* When time ranges of taxa that can be accurately calibrated (as in Europe and North America) are considered, these fit better with the order of nodes in the monophyletic equoid alternative. The paraphyletic equoid alternatives show equoid ghost lineages inversely proportional in length to their closeness of relationships. Other lines of evidence also favor the monophyletic equoid alternative. The functionless vestigial upper molar mesostyle of the otherwise bilophodont *Cardiolophus* indicates a rapid shift from dilambdodonty to bilophodonty early in perissodactyl evolution (Hooker, 1989). Moreover, *Hyracotherium,* with its posterior optic foramen and incipiently deepening narial incision is best viewed as the initiation of the family Palaeotheriidae (Hooker, 1994) rather than as the first step away from dilambdodonty. Froehlich's (1999) analysis showed *Cymbalophus* as a tapiromorph, not an equoid, and contrasts with the results obtained here. This may be a shortcoming of not combining clearly linked upper and lower tooth characters, so inadvertently weighting certain features.

The maximum parsimony cladogram that best fits the stratigraphic ranges of taxa, by having the shortest ghost ranges, is shown with character state changes in Figure 12. It shows the next branch to split off above the brontotheres to be the family Isectolophidae, comprising *Cardiolophus* and *Orientolophus.* Above this is a clade consisting of equoids (with *Cymbalophus* at its stem) and *Pachynolophus* plus *Karagalax.* The main characters defining this entire clade are: Reduction of the upper molar parastyle, lengthening of upper molar postmetacrista and of occlusally related lower molar paracristid, and lengthening of the postcanine diastema. These characters are shared by both equoids and ceratomorphs. *Pachynolophus* and *Karagalax* lack equoid characters but share a tall P_3 paraconid and are interpreted here as very primitive ceratomorphs. This contrasts with Maas et al. (2001) who placed *Karagalax* in the Isectolophidae.

Figure 13 shows this cladogram placed on an early Eocene paleogeographic map, and Figure 14 the postulated dispersal events that are listed below:

1. A crossing of the Bering Straits by *Ectocion* in the late Paleocene leading, via *Lophocion,* to origin and initial radiation of the perissodactyls.
2. Dispersal to Europe, via the Turgai Straits in the latest Paleocene.
3. Origin of equoids in Europe before the beginning of the Eocene.
4. Dispersal of equoids to N. America in two phases early in the Eocene.
5. Subsequent colonizations of North America by isectolophids (*Cardiolophus*), ceratomorphs (*Heptodon, Hyrachyus*) and brontotheriids (*Lambdotherium, Eotitanops*), in that order, via the Bering Straits in the course of the early Eocene.
6. Dispersal to the Indian subcontinent sometime in the early Eocene.

Downloaded from specialpapers.gsapubs.org on June 4, 2015

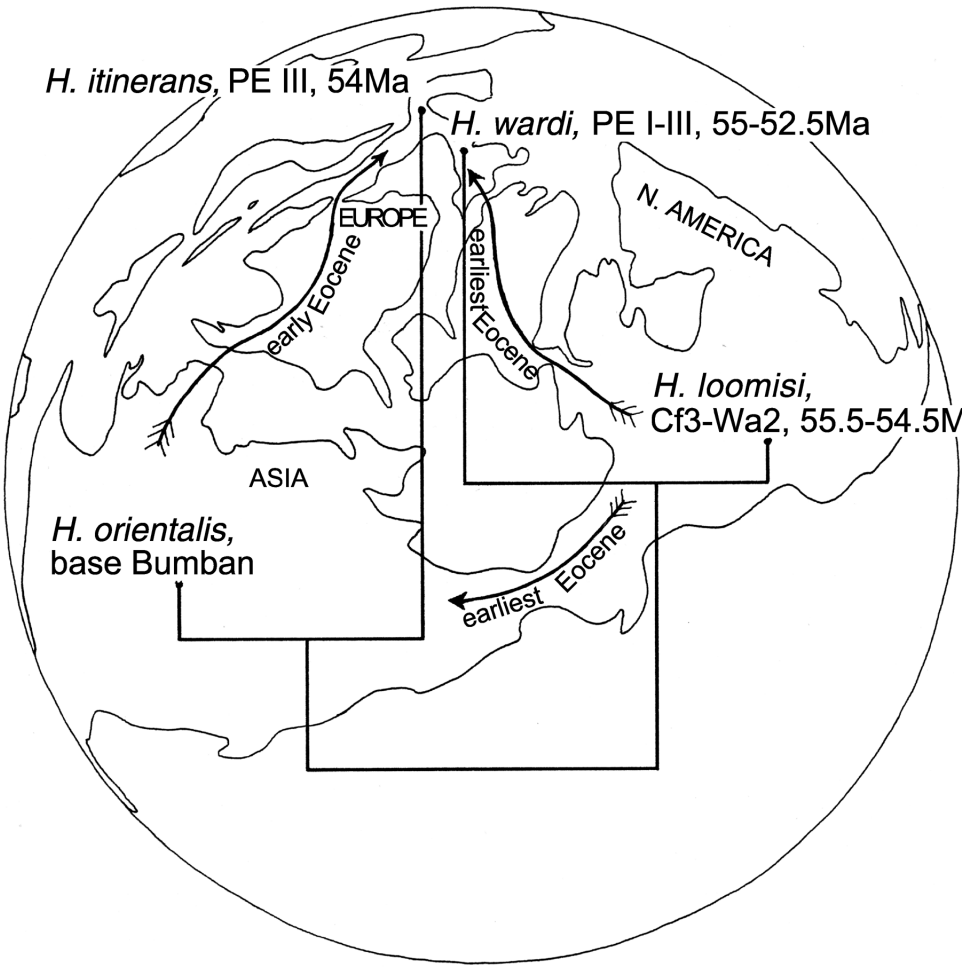

Figure 10. Early Eocene polar projection Northern Hemisphere paleogeographic shoreline map, with superimposed cladogram of early *Hyopsodus* species from Figure 2 with zones, time ranges in Ma where known and proposed dispersal directions (arrows) (map from unpublished work by Paul Markwick, see Markwick et al., 2000, with minor modifications to North Sea–Arctic Ocean link following Iakovleva et al., 2001).

Until *Lophocion* was described (Wang and Tong, 1997), the phenacodontids that are phenetically closest to perissodactyls were restricted to North America, an unlikely center of origin for the order Perissodactyla, in view of the sudden appearance there of only equoids and isectolophids at the beginning of the Eocene. The discovery of *Lophocion,* although young in age (contemporaneous with perissodactyls in the early Eocene Wutu Formation) makes the origin of perissodactyls in Asia a more tenable hypothesis. The fragmentary perissodactyl teeth from the Gashatan of Bayan Ulan, China (Meng et al., 1998), if really Paleocene (see Bowen et al., 2002), would represent the oldest perissodactyl. Although difficult to interpret because of breakage and heavy wear, they give the appearance of a *Lambdotherium*-like perissodactyl as Meng et al. (1998) proposed, but less dilambdodont. Thus, the upper molar centrocrista is slightly less buccally flexed and the lower preultimate molar hypoconulid is central rather than lingually displaced. Also, the entoconid seems not to be isolated as in *Orientolophus* and the more derived primitive equoids like *Pliolophus* and *Hyracotherium.* In these respects it is close to what would be expected of the basal perissodactyl.

THE TURGAI ROUTE AND TIMING OF DISPERSALS

The three examples above provide evidence of east to west dispersal between Asia and Europe as well as a model for origin and early evolutionary history of the order Perissodactyla. Similar treatments could help elucidate the origins of other enigmatic Eocene newcomers such as primates and artiodactyls. According to paleogeographic reconstructions (e.g., McKenna, 1975), the most likely crossing point was the Turgai Straits.

Iakovleva et al. (2001), in a study of combined dinocyst and sequence stratigraphy in the Turgai area, have indicated four hiatuses in the succession, relating to intervals of low sea level during the late Paleocene (Thanetian) and earliest Eocene (early Ypresian). These could have bridged the Turgai Straits, thus allowing terrestrial dispersal. They are (1) between 57.2 and 57.4 Ma (early Thanetian); (2) between 56.4 and 57.1 Ma (mid Thanetian); (3) between 55 and 55.1 Ma (late Thanetian, just before the CIE); and (4) between 54 and 54.5 Ma (early Ypresian). The time scale is that of Berggren et al. (1995) calibrated to dinocyst zonations and sequence stratigraphy via Hardenbol et al. (1998), Mudge and Bujak (1996) and Powell

Downloaded from specialpapers.gsapubs.org on June 4, 2015

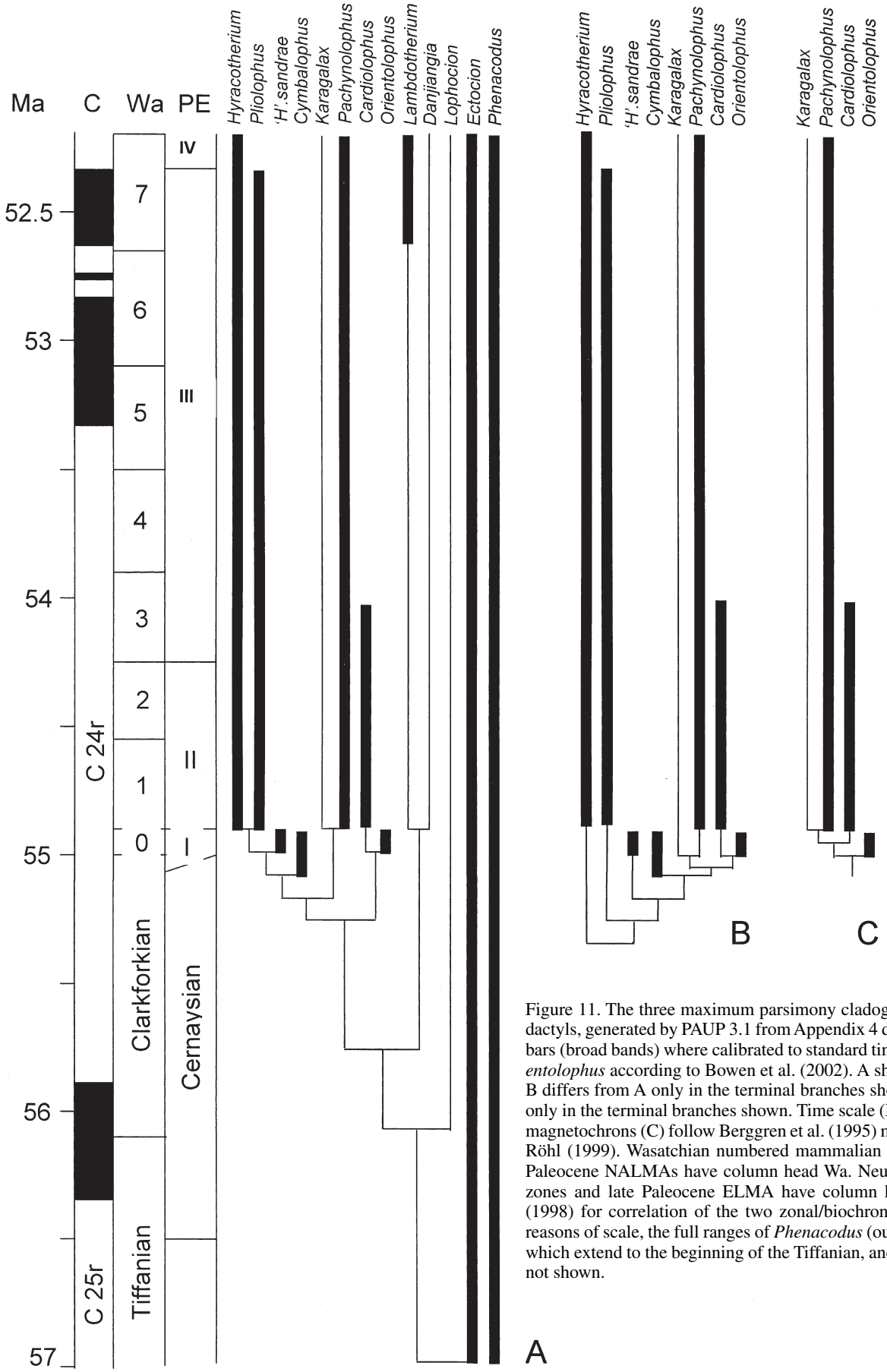

Figure 11. The three maximum parsimony cladograms of stem perissodactyls, generated by PAUP 3.1 from Appendix 4 data matrix, with range bars (broad bands) where calibrated to standard time scale; range of *Orientolophus* according to Bowen et al. (2002). A shows a full cladogram; B differs from A only in the terminal branches shown; C differs from B only in the terminal branches shown. Time scale (Ma) and calibration of magnetochrons (C) follow Berggren et al. (1995) modified by Norris and Röhl (1999). Wasatchian numbered mammalian Wa biozones and late Paleocene NALMAs have column head Wa. Neustrian mammalian PE zones and late Paleocene ELMA have column head PE. See Hooker (1998) for correlation of the two zonal/biochronological systems. For reasons of scale, the full ranges of *Phenacodus* (outgroup) and *Ectocion,* which extend to the beginning of the Tiffanian, and the basal branch, are not shown.

Downloaded from specialpapers.gsapubs.org on June 4, 2015

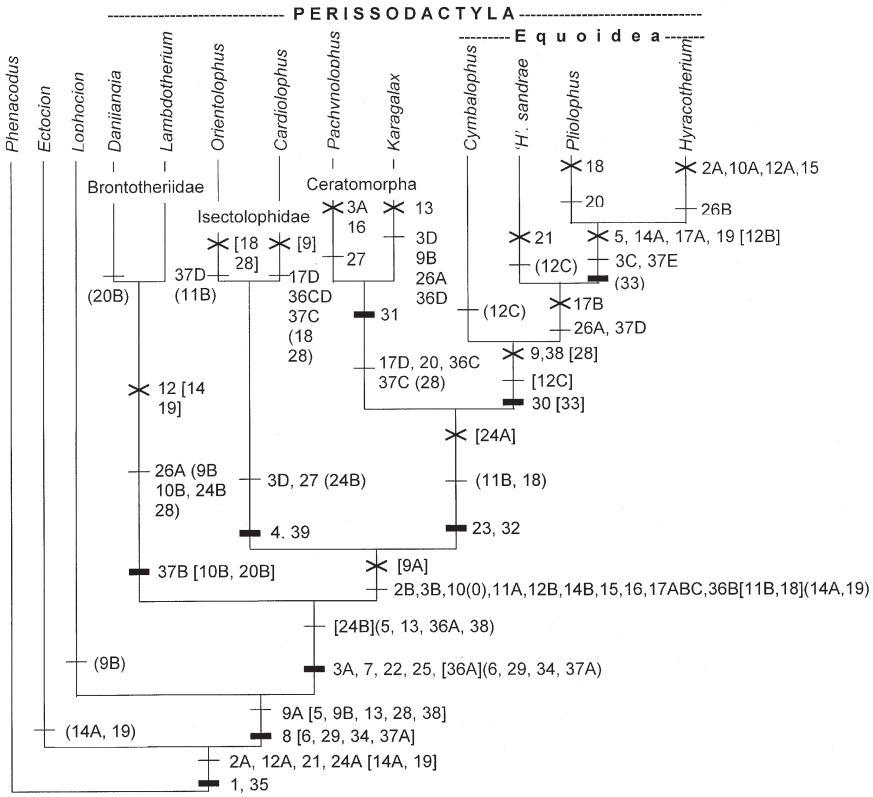

Figure 12. The maximum parsimony cladogram from Figure 11A, showing character state changes. See Appendix 3 for description of numbered characters, Appendix 4 for data matrix, and Figure 2 for explanation of notation.

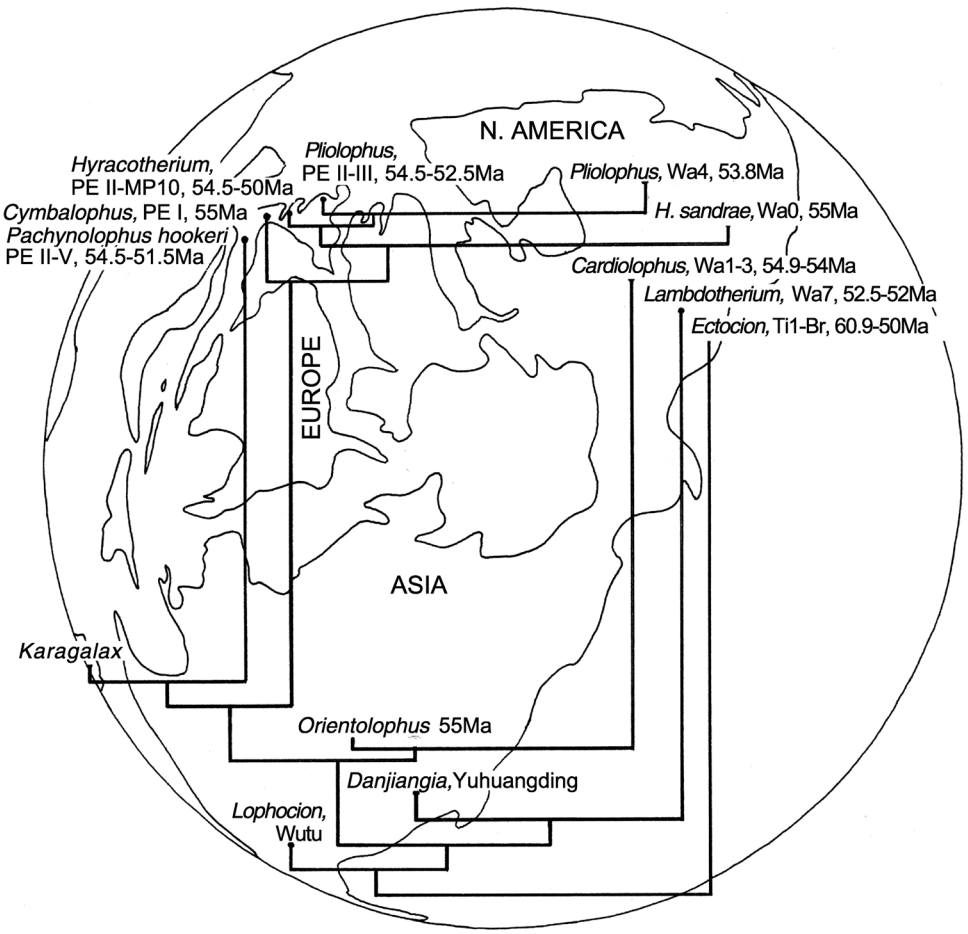

Figure 13. Early Eocene polar projection Northern Hemisphere paleogeographic shoreline map, with superimposed cladogram of stem perissodactyl and phenacodontid taxa from Figure 12 (map from unpublished work by Paul Markwick, see Markwick et al., 2000, with minor modifications to North Sea–Arctic Ocean link following Iakovleva et al., 2001). Zones and time ranges in Ma given where known, formational names given where dating uncertain.

Downloaded from specialpapers.gsapubs.org on June 4, 2015

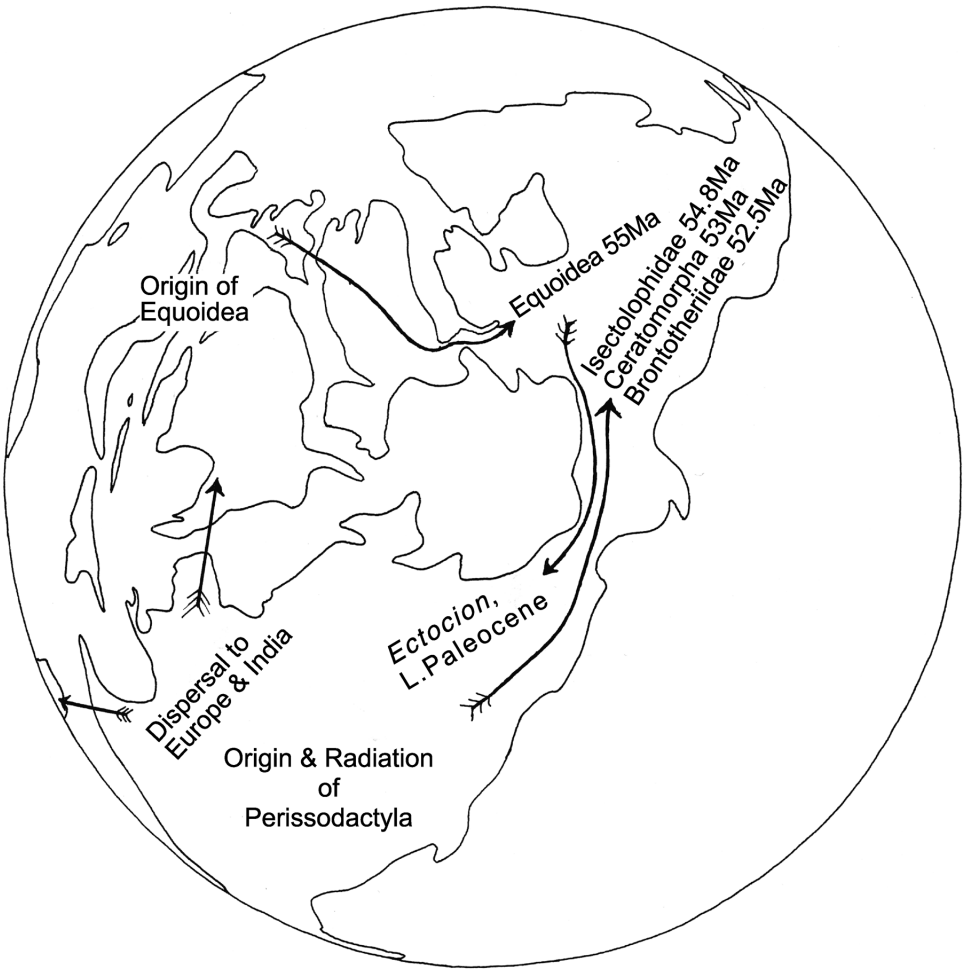

Figure 14. Same map as in Figure 13, with proposed dispersal directions and timings (arrows) for phenacodontids and stem perissodactyls.

et al. (1996), modified around the CIE according to Norris and Röhl (1999).

If the Bumbanian ALMA indeed extends no earlier than early Eocene (Bowen et al., 2002) and if the occurrence at Tsagan Khushu of *Lessnessina khushuensis* approximates the appearance of the genus in Asia, then hiatuses 1–3 are too early to be the ones allowing dispersal of *Lessnessina* to Europe. The earliest occurrence of the genus in Europe in mammal zone PE III (Hooker, 1998), however, fits closely with hiatus 4. It is therefore likely that *Lessnessina* crossed the Turgai Straits to Europe ~54.5 Ma, shortly before its appearance at Abbey Wood.

The same arguments apply to the Mongolian (Bumbanian) and southern French (PE III) occurrences of *Hyopsodus. Hyopsodus* is thus also likely to have crossed the Turgai Straits early in the timespan of hiatus 4, perhaps at ~54.5 Ma.

Perissodactyls including equoids have their first appearance in northwest Europe at around the MDE (Hooker, 1994, 1998). Differentiation of equoids must have taken place within Europe (although apparently not in the northwest) prior to this, but there is currently no record of it. Hiatus 3, which immediately predates the CIE, hardly allows time for this differentiation prior to the equoid first appearance in PE I (Hooker, 1994, 1998). Late in the long hiatus 2 (e.g., ~56.5 Ma) thus is the most likely interval for a perissodactyl crossing of the Turgai Straits. This has the feeling of being "too early," bearing in mind our near total lack of knowledge of this order before the beginning of the Eocene at 55 Ma. However, it provides a working hypothesis and a prediction that is testable by future discovery of the elusive late Paleocene perissodactyl record, which the cladistic analysis predicts to exist somewhere.

As the Turgai Straits are at mid latitudes, not high latitudes like the Bering and Greenland land bridges, it is unlikely that ameliorating climate was the driving force behind these three dispersals. Low sea level providing either a narrow land bridge or a greatly narrowed strait, allowing relatively easy rafting, is the scenario that seems best to fit the current evidence.

ACKNOWLEDGMENTS

We thank Dr. Paul Markwick for allowing us to use outlines of his unpublished paleogeographic maps; Dr. Philip Gingerich for providing measurements of the *Hyopsodus loomisi* teeth used

Downloaded from specialpapers.gsapubs.org on June 4, 2015

herein and, together with Drs. Don Russell, Marc Godinot, Spencer Lucas, and Hans Thewissen, casts of relevant specimens; and Dr. Adrian Rundle, Messrs. David Bone, Brian Gasson, Allan Lawson, Bill Morris and David Ward, for presenting important Abbey Wood mammals to the Natural History Museum, London. Ms. Pat Hart and Messrs. Harry Taylor and Kevin Webb of the NHM Photostudio ably composed the photographic illustrations. Prof. Bill Clemens provided helpful discussion on hyopsodontids. Comments by Spencer Lucas and an anonymous reviewer improved the manuscript. We are grateful to The Royal Society for funding visits to Mongolia and England. This is a contribution to the NHM Human Origins Programme, project 298.

APPENDIX 1. HYOPSODONTID CHARACTER DESCRIPTIONS

Description of characters used in the hyopsodontid cladistic analysis (see text and data matrix in Appendix 2). Multistate characters are ordered, representing linear transformation series. 0 is primitive state except for characters 1, 5, and 17, where A is primitive state and 0 is derived. 1 is derived state for binary characters. A, B, C, and D are otherwise derived states of multistate characters.

Character 1: Lower molar paraconid, small, distinctly separate from metaconid (0); tall, distinctly separate from metaconid (A) PRIMITIVE; tall, close to metaconid (B); fused to metaconid on $M_{2–3}$ (C).

Character 2: Upper molars with precingulum extending to lingual wall of tooth (0); precingulum with protostyle extending on M^1 two thirds to three quarters the distance to the lingual wall (1).

Character 3: P_4 with paracristid weak (0); strong (1).

Character 4: P_4 with distal protoconid crest weak (0); strong (1).

Character 5: P_4 without metaconid (0); with small metaconid (A) PRIMITIVE; with large metaconid (B).

Character 6: P^4 without metacone and with short protocone, P_4 without basined talonid (0); P^4 with faint metacone and short protocone, P_4 with short basined talonid (A); P^4 with faint metacone and long protocone, P_4 with long basined talonid (B); P^4 with small distinct metacone and long protocone, P_4 with long basined talonid with subterminal hypoconid (C); P^4 with small distinct metacone and long protocone, P_4 with long basined talonid with subterminal hypoconid and distinct entoconid (D).

Character 7: P_4 with distal talonid cusp(s) low (0); tall (1).

Character 8: P_4 with paraconid (or its position on the mesial end of the paracristid) half the height of the protoconid or less (0); taller (1).

Character 9: Upper molars with parastyle and ectocingulum strong (0); weak (1).

Character 10: Upper molar mesostyle absent (0); present (1).

Character 11: Upper molar postprotocingulum absent (0); present (1).

Character 12: M_3 larger than M_2 (0); M_3 and M_2 subequal (A); M_3 slightly smaller than M_2 (B); M_3 much smaller than M_2 (C). E.g., Figure 9.

Character 13: Lower preultimate molar hypoconulid nearly median (0); distinctly displaced lingually (1).

Character 14: Lower molar paracristid with rounded mesiobuccal corner (0); with sharp mesiobuccal corner (1).

Character 15: Upper molars with low protocone, lower molars with tall entoconid (0); M^2 with tall protocone, M_2 with low entoconid (A); all upper molars with tall protocone, all lower molars with low entoconid (B).

Character 16: Lower molar paraconid-metaconid complex and protoconid subequal in height (0); paraconid-metaconid complex distinctly taller (1).

Character 17: Lower molar cristid obliqua contact with back of trigonid lingual of midline (0); more or less median (A) PRIMITIVE; more buccal (B).

Character 18: Lower molar protocristid shallowly notched (0); deeply notched or missing (1).

Character 19: Molar cresting weak (0); strong (1).

Character 20: Crown height low (0) (e.g., Figure 7B–C); higher (1) (e.g., Figure 7G).

Character 21: P^4 with mesial parastyle projection strong (0); weak (1).

Character 22: Lower molar entocristid present (0); absent (1).

Character 23: Mesial and distal contact walls of adjacent lower molars transverse (0); oblique (1).

Character 24: Lower preultimate molar hypoconulid poorly differentiated from postcristid (0) (e.g., Figure 1G); well differentiated from postcristid (1) (e.g., Figure 6A).

APPENDIX 2. HYOPSODONTID DATA MATRIX

Data matrix for hyopsodontids derived from characters in Appendix 1. *Protungulatum* is outgroup taxon.

Taxon	111111111122222 123456789012345678901234
Protungulatum	A000A00000000000A0000000
Protoselene	0111AC0101001000A0000001
Dorraletes	0101AD01000C1000A0000000
Haplomylus	0101AD01101C1000A0000000
Promioclaenus	B111AA00000A0000A0000000
Litaletes	B111BA10000A00A0A0000000
Lessnessina khushuensis	B??????????A01B1B100?000
Lessnessina packmani	C1110010110?01B1B1000000
Lessnessina praecipuus	C?110011???C01B1B110?000
Hyopsodus loomisi/wardi	C111BB00100A0000A0001011
Hyopsodus orientalis	C111BA00100B100000010111
Hyopsodus itinerans	C111BA00100C10000001?111

Downloaded from specialpapers.gsapubs.org on June 4, 2015

APPENDIX 3. PERISSODACTYL CHARACTER DESCRIPTIONS

Description of characters used in the perissodactyl cladistic analysis (see text and data matrix in Appendix 4). These follow, with modifications and additions, those used by Hooker (1994). Multistate characters are fully ordered, except for 3 and 37, which are partially ordered and coded as stepmatrices. 0 is primitive state except for characters 10 and 20, where A is primitive state and 0 is derived. 1 is derived state for binary characters. A, B, C, D, and E are otherwise derived states of multistate characters.

Character 1: Cheek teeth generally bunodont with cresting weak (0); more strongly crested, with tendency to form ectoloph on upper molars (1).

Character 2: Upper molar preparaconule crista directed toward parastyle (0); toward preparacrista, variably joining it (A); toward preparacrista, constantly joining it (B).

Character 3: Upper molar paraconule not mesially distanced from the protocone, lacking facet 2A, preprotocrista mesiobuccally directed toward the paraconule, lower molar metaconid single, bearing facets 2 and 3 (0); upper molar paraconule, with facet 2A, mesially distanced from protocone, preprotocrista mesiobuccally directed toward the paraconule, lower molar metaconid widely twinned, bearing facets 2, 2A and 3 (A); upper molar paraconule, with facet 2A, not mesially distanced from protocone, preprotocrista nearly buccally directed toward the paraconule, lower molar metaconid narrowly twinned, bearing facets 2, 2A and 3 (B); upper molar paraconule, with facet 2A, mesially distanced from protocone, preprotocrista buccally directed to just behind the paraconule, lower molar metaconid widely twinned, bearing facets 2, 2A and 3 (C); upper molar paraconule nearly in line with protocone, lacking facet 2A and facets 2 and 3 nearly merged, lower molar metaconid single, undivided facets 2 and 3 forming distal bevel (D). Stepmatrix:

	0	A	B	C	D
0	-	1	2	3	3
A	1	-	1	2	2
B	2	1	-	1	1
C	3	2	1	-	2
D	3	2	1	2	-

Character 4: Lower molar cristid obliqua straight (0); bowed buccally (1).

Character 5: Lower molar protolophid notched (0); shallowly indented, lophoid (1).

Character 6: Lower molar metastylid a prominent cuspule (0); weak to lacking (1).

Character 7: Upper molar metaconule situated on a line drawn between the metacone and hypocone, lower molar hypoconulid an integral part of the postcristid (0); upper molar metaconule (or its position if subsumed by metaloph) distinctly mesial of a line drawn between the metacone and hypocone, lower molar hypoconulid separated from and distal of crest joining hypoconid and entoconid (hypolophid) (1).

Character 8: Upper molar metaconule not joined to hypocone by crest (0); joined to hypocone by crest (1).

Character 9: Upper molar metaconule large (0); size variable, some large, some small (A); all small (B).

Character 10: Upper molar centrocrista straight (0); slightly flexed buccally (A) PRIMITIVE; sharply flexed buccally (B).

Character 11: Upper molar mesostyle large (0); small or variably developed (A); lacking (B).

Character 12: Lower molar buccal and lingual cusp outer walls converge at ~45° (0); ~20° (A); ~10° (B); ~5° (C).

Character 13: Lower molar metaconid butress (Hooker, 1994, Figure 2E–F) weak or absent (0); strong (1).

Character 14: Lower molar cristid obliqua attaches to trigonid nearer to metaconid than to protoconid (0); midway between protoconid and metaconid (A); nearer to protoconid than to metaconid (B).

Character 15: Lower molar cristid obliqua attachment on back wall of trigonid, high (0); low (1).

Character 16: Lower molar entoconulid a prominent cuspule (0); weak to lacking (1).

Character 17: Lower molar paracristid, when lightly worn, makes angle to tooth long axis of 50° (0); 40° (A); 30° (B); 20° (C); 10° (D).

Character 18: Lower molar paracristid with mesiobuccal angle rounded (0); sharp or bulging (1).

Character 19: Lower molar trigonid back wall shallow (0); steep (1).

Character 20: P_{1-2} diastema absent (0); short (A) PRIMITIVE; long (B).

Character 21: M^{1-2} as long as broad (0); broader than long (1).

Character 22: M^3 without hypocone (0); with hypocone (1).

Character 23: Upper molar postmetacrista and lower molar paracristid buccal segment short (0); long (1).

Character 24: Upper molar parastyle small (0); medium (A); large (B).

Character 25: M^3 smaller than M^2, M_3 not larger than M_2 (0); M^3 not smaller than M^2, M_3 larger than M_2 (1).

Character 26: M_3 hypoconulid as close to hypoconid as this is to entoconid (0); more distant but closer to hypoconid than this is to protoconid (A); as far or further from hypoconid than this is from protoconid (B).

Character 27: M_3 hypoconulid forming distal margin of posttalonid lobe (0); bearing more distal lobe (1).

Character 28: M_3 hypolophid incomplete (0); complete (1).

Character 29: P^3 metacone smaller than paracone (0); as large as paracone (1).

Character 30: P^3 with trigon relatively narrow, protoloph weak, paraconule and P_3 metaconid very small and poorly defined (0); trigon broader, protoloph stronger, paraconule and metaconid much larger and better defined, but smaller than protocone and protoconid respectively (1).

Downloaded from specialpapers.gsapubs.org on June 4, 2015

Character 31: P_3 paraconid weak and much lower than protoconid (0); strong and approaching height of protoconid (1).
Character 32: Lower canine to P_1 diastema short (0); long (1).
Character 33: Optic foramen of orbit significantly in front of (0) or close to (1) anterior lacerate foramen (1). [N.B. *Ectocion* recoded following Holbrook (2001, p. 16–17).]
Character 34: Navicular facet of astragalus convex (0); saddle-shaped (1).
Character 35: Astragalar canal present (0); absent (1).
Character 36: Upper molars with no metaloph (0); with metaconal fold (Hooker, 1994, Figure 2A–C) not joined to metaconule (A); some joined to metaconule, some not (B); consistently joined to metaconule forming complete metaloph (C); buccal end of metaloph (homologue of metaconal fold) shifted mesially from metacone (D).
Character 37: Lower molar without hypolophid (0); hypolophid complete, comprising equal buccal and lingual segments of former postcristid joining in middle at notch in front of hypoconulid (A); buccal segment lengthened at expense of lingual segment with lingual hypoconulid (B); equal buccal and lingual segments joined into strong unnotched loph, hypoconulid median (C); hypolophid notched but complete like state A, some with lingual segment broken (D); hypolophid with lingual segment consistently broken (E). Step-matrix:

	0	A	B	C	D	E
0	-	1	2	2	2	3
A	1	-	1	1	1	2
B	2	1	-	2	2	3
C	2	1	2	-	2	3
D	2	1	2	2	-	1
E	3	2	3	3	1	-

Character 38: Lower $M_{1–2}$ distal cingulum lingual of hypoconulid absent (0); present (1).
Character 39: Upper molar protoloph and metaloph and lower molar protolophid and hypolophid transverse (0); oblique (1).

APPENDIX 4. PERISSODACTYL DATA MATRIX

Data matrix for perissodactyls and related phenacodontids derived from characters in Appendix 3. N.B. *Hyracotherium* indicates only the type species *H. leporinum* (see Hooker, 1994). *Pachynolophus* involves mainly the most primitive species (*P. hookeri* Godinot in Godinot et al., 1987), but also others for skull characters (Remy, 1972; Savage et al., 1965) and other pachynolophids for postcranial characters (Depéret, 1917). Data from original material, casts and, in the case of *Danjiangia* and *Lophocion,* from the literature (Wang, 1995; Wang and Tong, 1997). Relevant additional sources are: Gingerich (1989, 1991), Thewissen (1990) and Ting (1993).

Taxon	11111111112222222222333333333312345678901234567890123456789012345678901234567890123456789
Hyracotherium	1AC001110ABA1A01A10A111A1B0011?11??BE00
Cymbalophus	1BB0111100BC1B11C11A111A10001101???BA00
"H." sandrae	1BB0111100BC1B11B11A011A1A001101?11BD00
Cardiolophus	1BD11111A0AB1B11D11A110B10111000?11DC11
Orientolophus	1BD11111A0BB1B11C01?1?0B1010???????BD11
Lambdotherium	1AA01111BB001000000?110B1A01100??11AB10
Danjiangia	1AA01111BB001000000B110B1A011000???AB?0
Lophocion	1A0???01BA0A????????100A0??????????0??0
Ectocion	1A0000000A0A0A00001A100A000000000010000
Karagalax	1BD01111B0BB0B11D110111A1A011011?11DC10
Pachynolophus	1BA01111A0BB1B10D110111A10111011011CC10
Pliolophus	1BC0011100BB1A11A000111A1A001101111BE00
Phenacodus	000000000A000000000A0000000000000000000

REFERENCES CITED

Archibald, J.D., 1998, Archaic ungulates ("Condylarthra"), *in* Janis, C.M., et al., eds., Evolution of Tertiary mammals of North America, volume 1: Terrestrial carnivores, ungulates, and ungulatelike mammals: Cambridge, UK, Cambridge University Press, p. 292–331.

Archibald, J.D., Rigby, J.K., Jr., and Robison, S.F., 1983, Systematic revision of *Oxyacodon* (Condylarthra, Periptychidae) and a description of *O. ferronensis* n. sp.: Journal of Paleontology, v. 57, p. 53–72.

Beard, K.C., 1998, East of Eden: Asia as an important center of taxonomic origination in mammalian evolution: Bulletin of Carnegie Museum of Natural History, v. 34, p. 5–39.

Beard, K.C., and Dawson, M.R., 1999, Intercontinental dispersal of Holarctic land mammals near the Paleocene-Eocene boundary: Paleogeographic, paleoclimatic and biostratigraphic implications: Bulletin de la Société Géologique de France, v. 170, p. 697–706.

Berggren, W.A., Kent, D.V., Swisher, C.C., III, and Aubry, M.-P., 1995, A revised Cenozoic geochronology and chronostratigraphy, *in* Berggren, W.A., et al., eds., Geochronology, time scales, and global stratigraphic correlation: SEPM (Society for Sedimentary Geology) Special Publication 54, p. 129–212.

Bowen, G.B., Clyde, W.C., Koch, P.L., Ting Suyin, Alroy, J., Tsubamoto, Takehisa, Wang Yuanqing, and Wang Yuan, 2002, Mammalian dispersal at the Paleocene–Eocene boundary: Science, v. 295, p. 2062–2065.

Butler, P.M., 1972, Some functional aspects of molar evolution: Evolution, v. 26, p. 474–483.

Butler, P.M., 1973, Molar wear facets of early Tertiary North American primates, *in* Zingeser, M.R., ed., Craniofacial biology of primates: Symposia of the Fourth International Congress of Primatology, Portland, Oregon, August 15–18, 1972, v. 3, p. 1–27.

Clyde, W.C., and Gingerich, P.D., 1998, Mammalian community response to the latest Paleocene thermal maximum: An isotaphonomic study in the northern Bighorn Basin, Wyoming: Geology, v. 26, p. 1011–1014.

Cope, E.D., 1881, A new type of Perissodactyla: American Naturalist, v. 15, p. 1017–1018.

Crompton, A.W., and Kielan-Jaworowska, Z., 1978, Molar structure and occlusion in Cretaceous therian mammals, *in* Butler, P.M., and Joysey, K.A., eds., Studies in the development, function and evolution of teeth: London, Academic Press, p. 249–287.

Dashzeveg, D., 1977, On the discovery of *Hyopsodus* Leidy, 1870 (Mammalia, Condylarthra) in the Mongolian People's Republic, *in* Barsbold, R., and Vorobjeva, E.L., eds., Mesozoic and Cenozoic faunas, floras and biostratigraphy of Mongolia: Trudy Sovmestnaya Sovetsko-Mongol'skaya Paleontologicheskaya Ekspeditsiya, v. 4, p. 7–13.

Depéret, C., 1910, Etudes sur la famille des lophiodontidés: Bulletin de la Société Géologique de France, ser. 4, v. 10, p. 558–577.

Downloaded from specialpapers.gsapubs.org on June 4, 2015

Depéret, C., 1917, Monographie de la faune de mammifères fossiles du Ludien inférieur d'Euzet-les-Bains (Gard): Annales de l'Université de Lyon, new series, I Sciences, Médecine, v. 40, p. 1–290.

Estravis, C., and Russell, D.E., 1992, The presence of Taeniodonta (Mammalia) in the early Eocene of Europe: Ciências da Terra (Universidade Nova de Lisboa), v. 11, p. 191–201.

Forey, P.L., Humphries, C.J., Kitching, I.J., Scotland, R.W., Siebert, D.J., and Williams, D.M., 1992, Cladistics, a practical course in systematics: Systematics Association Publication No. 10: Oxford, Clarendon Press, 191 p.

Froehlich, D.J., 1999, Phylogenetic systematics of basal perissodactyls: Journal of Vertebrate Paleontology, v. 19, p. 140–159.

Gingerich, P.D., 1974, Stratigraphic record of early Eocene *Hyopsodus* and the geometry of mammalian phylogeny: Nature, v. 248, p. 107–109.

Gingerich, P.D., 1976a, Paleontology and phylogeny: Patterns of evolution at the species level in early Tertiary mammals: American Journal of Science, v. 276, p. 1–28.

Gingerich, P.D., 1976b, Cranial anatomy and evolution of early Tertiary Plesiadapidae (Mammalia, Primates): University of Michigan Papers on Paleontology, v. 15, p. 1–141.

Gingerich, P.D., 1985, Species in the fossil record: Concepts, trends, and transitions: Paleobiology, v. 11, p. 27–41.

Gingerich, P.D., 1989, New earliest Wasatchian mammalian fauna from the Eocene of northwestern Wyoming: Composition and diversity in a rarely sampled high-floodplain assemblage: University of Michigan Papers on Paleontology, v. 28, p. 1–97.

Gingerich, P.D., 1991, Systematics and evolution of early Eocene Perissodactyla (Mammalia) in the Clarks Fork Basin, Wyoming: Contributions from the Museum of Paleontology, University of Michigan, v. 28, p. 181–213.

Godinot, M., 1978, Diagnoses de trois nouvelles espèces de mammifères du Sparnacien de Provence: Compte Rendu Sommaire des Séances de la Société Géologique de France, v. 1978, p. 286–288.

Godinot, M., 1981, Les mammifères de Rians (Eocène inférieur, Provence): Palaeovertebrata, v. 10, p. 43–126.

Godinot, M., Crochet, J.-Y., Hartenberger, J.-L., Lange-Badré, B., Russell, D.E., and Sigé, B., 1987, Nouvelles données sur les mammifères de Palette (Eocène inférieur, Provence): Münchner Geowissenschaftliche Abhandlungen, ser. A, v. 10, p. 273–288.

Hardenbol, J., Thierry, J., Farley, M.B., Jacquin, T., De Graciansky, P.-C., and Vail, P.R., 1998, Mesozoic and Cenozoic sequence chronostratigraphic framework of European basins: SEPM (Society for Sedimentary Geology) Special Publication 60, p. 3–13, 763–781.

Holbrook, L.T., 2001, Comparative osteology of early Tertiary tapiromorphs (Mammalia, Perissodactyla): Zoological Journal of the Linnean Society, v. 132, p. 1–54.

Hooker, J.J., 1979, Two new condylarths (Mammalia) from the early Eocene of southern England: Bulletin of the British Museum (Natural History), Geology series, v. 32, p. 43–56.

Hooker, J.J., 1986, Mammals from the Bartonian (middle/late Eocene) of the Hampshire Basin, southern England: Bulletin of the British Museum (Natural History), Geology series, v. 39, p. 191–478.

Hooker, J.J., 1989, Character polarities in early Eocene perissodactyls and their significance for *Hyracotherium* and infraordinal relationships, *in* Prothero, D.R., and Schoch, R.M., eds., The evolution of perissodactyls: New York, Oxford University Press, p. 79–101.

Hooker, J.J., 1994, The beginning of the equoid radiation: Zoological Journal of the Linnean Society, v. 112, p. 29–63.

Hooker, J.J., 1998, Mammalian faunal change across the Paleocene-Eocene transition in Europe, *in* Aubry, M.-P., et al., eds., Late Paleocene–early Eocene climatic and biotic events in the marine and terrestrial records: New York, Columbia University Press, p. 428–450.

Hooker, J.J., 2000, Ecological response of mammals to global warming in the late Paleocene and early Eocene: GFF, v. 122, p. 77–79.

Iakovleva, A.I., Brinkhuis, H., and Cavagnetto, C., 2001, Late Paleocene–early Eocene dinoflagellate cysts from the Turgay Strait, Kazakhstan: Correlations across ancient seaways: Palaeogeography, Palaeoclimatology, Palaeoecology, v. 172, p. 243–268.

Kondrashov, P.E., and Agadjanian, A.K., 1999, New material on the genus *Hyopsodus* (Mammalia, Condylarthra) from the Eocene of Mongolia: Morphological variability and taxonomic position: Paleontological Journal, v. 33, p. 667–676.

Krause, D.W., and Maas, M.C., 1990, The biogeographic origins of late Paleocene–early Eocene mammalian immigrants to the western interior of North America: Boulder, Colorado, Geological Society of America Special Paper 243, p. 71–105.

Leidy, J., 1870, Remarks on a collection of fossils from the western territories: Proceedings of the Academy of Natural Sciences, Philadelphia, v. 22, p. 109–110.

Lipscomb, D.L., 1992, Parsimony, homology and the analysis of multistate characters: Cladistics, v. 8, p. 45–65.

Maas, M.C., Hussain, S.T., Leinders, J.J.M., and Thewissen, J.G.M., 2001, A new isectolophid tapiromorph (Perissodactyla, Mammalia) from the early Eocene of Pakistan: Journal of Paleontology, v. 75, p. 407–417.

Markwick, P.J., Rowley, D.B., Ziegler, A.M., Hulver, M.L., Valdes, P.J., and Selwood, B.W., 2000, Late Cretaceous and Cenozoic global palaeogeographies: Mapping the transition from a "hot-house" to an "ice-house" world: GFF, v. 122, p. 103.

Matthew, W.D., 1937, Paleocene faunas of the San Juan Basin, New Mexico: Transactions of the American Philosophical Society, v. 30, p. 1–510.

McKenna, M.C., 1960, Fossil mammalia from the early Wasatchian Four Mile fauna, Eocene of northwest Colorado: Berkeley, California, University of California Publications in Geological Science, v. 37, p. 1–130.

McKenna, M.C., 1975, Fossil mammals and early Eocene North Atlantic land continuity: Annals of the Missouri Botanical Garden, v. 62, p. 335–353.

McKenna, M.C., Chow Minchen, Ting Suyin, and Luo Zhexi, 1989, *Radinskya yupingae,* a perissodactyl-like mammal from the late Paleocene of China, *in* Prothero, D.R., and Schoch, R.M., eds., The evolution of Perissodactyls: New York, Oxford University Press, p. 24–36.

Meng Jin, Zhai Renjie, and Wyss, A.R., 1998, The late Paleocene Bayan Ulan fauna of Inner Mongolia, China: Bulletin of Carnegie Museum of Natural History, v. 34, p. 148–185.

Mudge, D.C., and Bujak, J.P., 1996, An integrated stratigraphy for the Paleocene and Eocene of the North Sea, *in* Knox, R.W.O'B., et al., eds., Correlation of the early Paleogene in northwest Europe: London, Geological Society Special Publication 101, p. 91–113.

Norris, R.D., and Röhl, U., 1999, Carbon cycling and chronology of climate warming during the Paleocene-Eocene transition: Nature, v. 401, p. 775–778.

Osborn, H.F., 1929, The titanotheres of ancient Wyoming, Dakota and Nebraska: Monographs of the U.S. Geological Survey, v. 55, p. 1–953.

Powell, A.J., Brinkhuis, H., and Bujak, J.P., 1996, Upper Paleocene–lower Eocene dinoflagellate cyst sequence biostratigraphy of southeast England, *in* Knox, R.W.O'B., et al., eds., Correlation of the early Paleogene in northwest Europe: London, Geological Society Special Publication 101, p. 145–183.

Radinsky, L.B., 1964, *Paleomoropus,* a new early Eocene chalicothere (Mammalia, Perissodactyla), and a revision of Eocene chalicotheres: American Museum Novitates, no. 2179, p. 1–28.

Radinsky, L.B., 1966, The adaptive radiation of the phenacodontid condylarths and the origin of the Perissodactyla: Evolution, v. 20, p. 408–417.

Redline, A.D., 1997, Revision of the Wind River faunas, early Eocene of central Wyoming, Part 13: Systematics and phylogenetic pattern of early Eocene *Hyopsodus* (Mammalia: Condylarthra): Annals of Carnegie Museum, v. 66, p. 1–81.

Remy, J.-A., 1972, Etude du crâne de *Pachynolophus lavocati* n. sp. (Perissodactyla, Palaeotheriidae) des Phosphorites du Quercy: Palaeovertebrata, v. 5, p. 45–78.

Rigby, J.K., Jr., 1980, Swain Quarry of the Fort Union Formation, middle Paleocene (Torrejonian), Carbon County, Wyoming: Geologic setting and mammalian fauna: Evolutionary Monographs, v. 3, p. 1–179.

Downloaded from specialpapers.gsapubs.org on June 4, 2015

Rose, K.D., 1981, The Clarkforkian Land-Mammal Age and mammalian faunal composition across the Paleocene-Eocene boundary: University of Michigan Papers on Paleontology, v. 26, p. 1–197.

Savage, D.E., Russell, D.E., and Louis, P., 1965, European Eocene Equidae (Perissodactyla): Berkeley, California, University of California Publications in Geological Science, v. 56, p. 1–94.

Savage, D.E., Russell, D.E., and Louis, P., 1966, Ceratomorpha and Ancylopoda (Perissodactyla) from the lower Eocene Paris Basin, France: Berkeley, California, University of California Publications in Geological Science, v. 66, p. 1–38.

Schoch, R.M., 1986, Systematics, functional morphology, and macroevolution of the extinct mammalian order Taeniodonta: Bulletin of the Peabody Museum of Natural History, v. 42, p. 1–307.

Simpson, G.G., 1937, The Fort Union of the Crazy Mountain Field, Montana and its mammalian faunas: Bulletin of the United States National Museum, v. 169, p. 1–287.

Sulimski, A., 1969, Paleocene genus *Pseudictops* Matthew, Granger and Simpson, 1929 (Mammalia) and its revision: Palaeontologia Polonica, v. 19, p. 101–131.

Swofford, D.L., 1990, PAUP: Phylogenetic Analysis Using Parsimony, Version 3.0: Computer program distributed by the Illinois Natural History Survey, Champaign, Illinois, 162 p.

Thewissen, J.G.M., 1990, Evolution of Paleocene and Eocene Phenacodontidae (Mammalia, Condylarthra): University of Michigan Papers on Paleontology, v. 29, p. 1–107.

Thewissen, J.G.M., and Domning, D.P., 1992, The role of phenacodontids in the origin of the modern orders of ungulate mammals: Journal of Vertebrate Paleontology, v. 12, p. 494–504.

Ting Suyin, 1993, A preliminary report on an early Eocene mammalian fauna from Hengdong, Hunan Province, China: Kaupia, v. 3, p. 201–207.

Trouessart, E.L., 1879, Catalogue des mammifères vivants et fossiles: Revue et Magazine de Zoologie, v. 7, p. 219–285.

Wang Jingwen, and Tong Yongsheng, 1997, A new phenacodontid condylarth (Mammalia) from the early Eocene of the Wutu Basin, Shandong: Vertebrata PalAsiatica, v. 35, p. 283–289.

Wang Yuan, 1995, A new primitive chalicothere (Perissodactyla, Mammalia) from the early Eocene of Hubei, China: Vertebrata PalAsiatica, v. 33, p. 138–159, 1 plate.

Williamson, T.E., 1996, The beginning of the Age of Mammals in the San Juan Basin, New Mexico: Biostratigraphy and evolution of Paleocene mammals of the Nacimiento Formation: Bulletin of the New Mexico Museum of Natural History and Science, v. 8, p. 1–141.

Xu Qinqi, 1976, New materials of Anagalidae from the Paleocene of Anhui (A): Vertebrata PalAsiatica, v. 14, p. 174–184.

Manuscript Accepted by the Society August 13, 2002

Printed in the USA

Downloaded from specialpapers.gsapubs.org on June 4, 2015

Geological Society of America Special Papers

Evidence for direct mammalian faunal interchange between Europe and Asia near the Paleocene-Eocene boundary

J. J. Hooker and D. Dashzeveg

Geological Society of America Special Papers 2003;369; 479-500
doi:10.1130/0-8137-2369-8.479

E-mail alerting services click www.gsapubs.org/cgi/alerts to receive free e-mail alerts when new articles cite this article

Subscribe click www.gsapubs.org/subscriptions to subscribe to Geological Society of America Special Papers

Permission request click www.geosociety.org/pubs/copyrt.htm#gsa to contact GSA.

Copyright not claimed on content prepared wholly by U.S. government employees within scope of their employment. Individual scientists are hereby granted permission, without fees or further requests to GSA, to use a single figure, a single table, and/or a brief paragraph of text in subsequent works and to make unlimited copies of items in GSA's journals for noncommercial use in classrooms to further education and science. This file may not be posted to any Web site, but authors may post the abstracts only of their articles on their own or their organization's Web site providing the posting includes a reference to the article's full citation. GSA provides this and other forums for the presentation of diverse opinions and positions by scientists worldwide, regardless of their race, citizenship, gender, religion, or political viewpoint. Opinions presented in this publication do not reflect official positions of the Society.

Notes

Geological Society of America

THE GEOLOGICAL SOCIETY OF AMERICA